Acta Mech 201, 131–151 (2008)
DOI 10.1007/s00707-008-0078-7

B. Scheichl · A. Kluwick · M. Alletto

"How turbulent" is the boundary layer separating from a bluff body for arbitrarily large Reynolds numbers?

Dedicated to Professor Wilhelm Schneider on the occasion of his 70th birthday

Received: 7 March 2008 / Revised: 15 May 2008 / Published online: 23 September 2008

Abstract The paper deals with separation of a nominally steady and two-dimensional incompressible boundary layer from the smooth surface of a rigid blunt body in the presence of a front stagnation point, here denoted by P_F. In agreement with earlier studies on the flow past a bluff body, it is argued that in the limit of vanishing viscosity, i.e. in the limit where the globally defined Reynolds number Re takes on arbitrarily large values, the solution of this problem is to be sought in the class of steady potential flows with free streamlines. Hence, it is first assumed that for sufficiently large values of Re the boundary layer upstream of separation is a fully developed turbulent one. Accordingly, it is demonstrated numerically and analytically, by adopting asymptotic techniques, how the well-known laminar flow taking place close to P_F is gradually transformed into a fully developed turbulent boundary layer further downstream, which exhibits the well-established typical asymptotic two-layer splitting. However, as has been shown in a preceding study, this type of flow does not allow for a self-consistent rational description of separation, based on the nominally steady form of the equations of motion. From this result, supported by numerical and experimental evidence, the tentative but rather remarkable conclusion is drawn that the boundary layer along the smooth surface of a bluff body never attains a fully developed turbulent state, even in the limit $Re \to \infty$. Most important, these findings are seen to be independent of the choice of a specific turbulence closure.

1 Introduction and motivation

Flow separation from a more-or-less bluff body, i.e. one with diameters of comparable magnitude in and normal to the direction of the oncoming unperturbed stream sufficiently far ahead of the body, in the limit of large values of the globally formed Reynolds number Re not only represents an extremely challenging and long-standing unsolved problem in theoretical hydrodynamics but, needless to say, is also of great engineering relevance. For example, a profound understanding of the very basic physical mechanism underlying flow separation is important in order to allow for further substantial progress in the prediction of undesired separation from airfoils with moderate aspect ratios.

B. Scheichl (✉) · A. Kluwick · M. Alletto
Institute of Fluid Mechanics and Heat Transfer, Vienna University of Technology,
Resselgasse 3/E322, Vienna, Austria
E-mail: bernhard.scheichl@tuwien.ac.at

A. Kluwick
E-mail: alfred.kluwick@tuwien.ac.at

M. Alletto
E-mail: e0127243@student.tuwien.ac.at

In the present study we shall be concerned with a solid plane body of a typical half-diameter $\tilde{L}$, having an impermeable and perfectly smooth surface, and immersed in an otherwise perfectly uniform stream with velocity $\tilde{U}$ of an incompressible fluid of constant density $\tilde{\rho}$ and constant kinematic viscosity $\tilde{\nu}$, respectively. We then assume that

$$Re := \tilde{U}\tilde{L}/\tilde{\nu} \to \infty. \tag{1}$$

Note that, under the above assumptions, the real flow physics is uniquely determined by the value of the single parameter Re. With regard to the subsequent discussion of this flow configuration and the associated notations of characteristic points on the body surface, we refer to the sketch in Fig. 1a referring to the canonical case of the problem, namely, a circular cylinder with radius $\tilde{L}$ in uniform transverse flow.

If in the limit given by Eq. (1) the flow is taken to be strictly laminar and steady, the seminal local asymptotic theory developed by Sychev [14] and Smith [12], see also Sychev et al. [15], applies to the close vicinity of the position of separation. In these studies the flow in the limit of vanishing viscosity has to be sought in the class of irrotational flows with free streamlines which depart smoothly from the surface at the point denoted by P_D. In general, this Helmholtz–Kirchhoff-type flow is associated with a streamwise pressure gradient that tends to infinity immediately upstream of P_D, see e.g. Gurevich [2]. That singular behavior, commonly referred to as Brillouin–Villat (hereafter abbreviated as BV) singularity, then prevents an asymptotic description of separation of the boundary layer (BL) evolving from the front stagnation point, as the solution of the BL problem terminates further upstream in form of a well-known Goldstein singularity, which cannot be surmounted in a rational manner. Therefore, the position of P_D has to be moved sufficiently far upstream such that the BV singularity becomes asymptotically weak (with respect to the value of Re), which in turn allows for a successful treatment of the separation process on the basis of the local viscous/inviscid interaction process.

Unfortunately, however, one has to face the fact that both the flow pattern and the drag coefficient predicted by the above rigorous description of separation are apparently not in satisfactory agreement with the experimental findings: an extensive discussion of the flow field based on measurements of the steady flow past a circular cylinder for various values of Re is presented in [17]. The observed disagreement leads to two major concerns: first of all, the question whether the flow should indeed be regarded as steady and irrotational in the limit $Re \to \infty$, which is crucial, is still unsettled. Surprisingly, it has not attracted many researchers so far. Thus, this assumption still requires a sound confirmation; a first systematic attempt in this direction, adopting both the Navier–Stokes equations and scaling arguments that are based on intuitive physical reasoning, is made in Sect. 3.

The second and most serious objection, however, is raised against the widely believed issue that not only the separated shear flow but even the entire BL upstream of separation becomes fully turbulent for sufficiently large values of Re; for a survey on this topic see [17] and the references therein. Interestingly, detailed measurements of the attached BL flow are rare. As a result, also this hypothesis still lacks a convincing experimental evidence. Moreover, from the oil film flow visualizations of the streamline pattern close to the surface performed by Schewe [10] one can draw the—tentative—conclusion that the BL slightly upstream of separation still exhibits typical laminar-like characteristics, even for values of Re up to approximately 7.7×10^6, whereas separation triggers its rather rapid transition towards a fully developed turbulent free shear layer. In the present study we account for this observation by adopting the approach taken up by Neish and Smith [6]: the level of turbulence intensities in the BL shall not be fixed in advance but governed by a suitably introduced control parameter, say, T. The assumption of a fully turbulent initially attached BL then is captured by considering a suitable distinguished double limit: $T \to \infty$, $Re \to \infty$. However, as far as this latter case is concerned, it has been outlined quite recently, [7], that the typical asymptotic structure of a fully turbulent BL is incompatible with separation provoked by the BV singularity at P_D of the limiting potential flow. This conclusion holds for largely arbitrary positions of P_D when the BV singularity assumes a finite strength. Neish and Smith [6] circumvent that severe shortcoming by exploring the possibility of a strictly attached potential flow, granted that the entire BL is a fully turbulent one (we note that their rationale for these assumptions is neither in agreement with the arguments put forward here nor the present results). In their analysis, separation is expected to take place a (non-dimensional) distance of $O\left[(\ln Re)^{-1/2}\right]$ upstream of the rear stagnation point of the body. However, it has been demonstrated that the proposed local asymptotic splitting of the flow then is incompatible with that deduced from an asymptotic investigation of the full set of the Reynolds-averaged equations of motion [7]. Furthermore, the collapse of P_D with the rear stagnation point can be interpreted as the occurrence of a BV singularity having infinite strength [2,7]. The aforementioned inconsistency encountered when a fully turbulent BL is driven by a potential flow that yields a BV singularity of finite strength, see [7], is presumably met again if

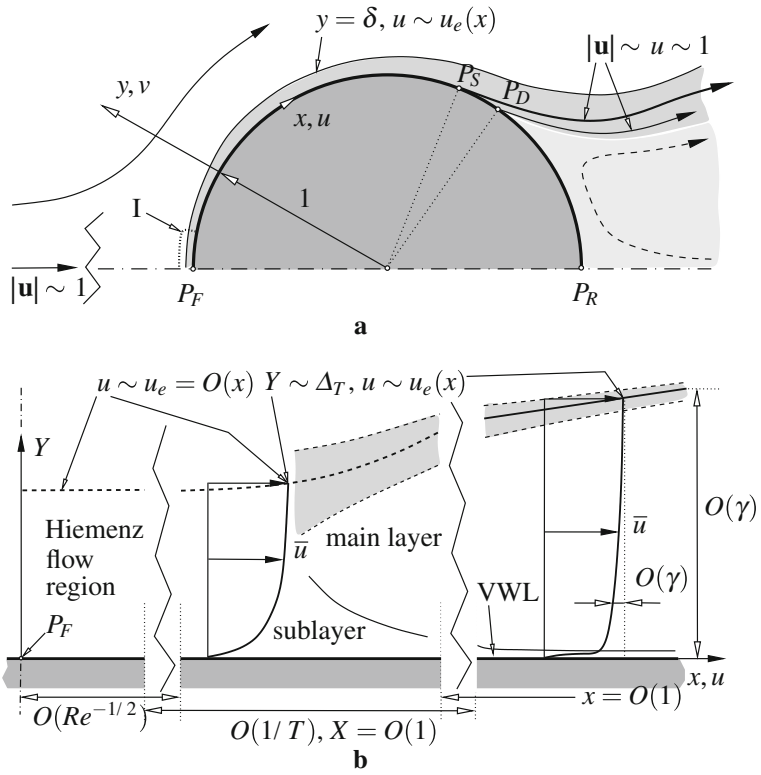

Fig. 1 **a** Flow configuration and natural coordinate system, shown for the case of a circular cylinder with non-dimensional radius 1, representing a bluff body with positive surface curvature $\varkappa(x)$: time-mean streamlines (*arrows* indicate flow direction), BL and separated shear layer (*dark-shaded*), streamlines of irrotational and viscous flow departing in P_D (*normal line*) and P_S (*bold line*), dividing the external flow from the zone with (almost stagnant) reverse flow (*light-shaded*). Separation is assumed to take place in the point P_S, i.e. slightly upstream of P_D, according to the flow picture in [6]. Transitional BL region I near P_F and BL splitting emerging for $T \to \infty$ is zoomed out in **b**, including the viscous wall layer VWL, and the viscous superlayer (*shaded*)

one considers the local flow structure resulting from a slight upstream shift of P_D. As a consequence, relaxing the assumption made in [6] that P_D takes on the form of a rear stagnation point only in the limit $Re \to \infty$ will also unlikely prove successful in establishing a self-consistent description of turbulent separation. In turn, we anticipate the remarkable preliminary result that the attached BL flow approaching separation has to be sought in the class of flows that prevail in a so-called transitional state, as they are neither laminar nor fully turbulent.

Hence, we draw the important conclusion that both a value of T and the position of P_D in the limit $Re \to \infty$ have to be chosen such that the solution of the BL equations meets the necessary requirements of matching with the flow quantities in the region in the immediate vicinity of separation, where the classical BL approximation of the governing equations ceases to be valid. That is, the asymptotic flow structure near separation presumably fixes the value of T, which provides the answer to the question, raised in the paper title, of "how turbulent" is the BL that stretches from the front stagnation point P_F to the position of separation. That flow picture in the limit (1) then strikingly contrasts that proposed by the theory of laminar separation epitomised above. Nevertheless, it agrees fairly well with that inferred from the experiments carried out by Tsahalis and Telionis [16]. These indicate that the observed distinctive deceleration of a turbulent BL closely upstream of separation points to a finite strength of the BV singularity of the limiting potential flow. Moreover, they relate the associated local behavior of the advective terms in the streamwise momentum equation to the occurrence of a pronounced Goldstein singularity if a BL approximation is adopted. Most important, the experimental data indicate that both singularities are characterized by a variation of the streamwise velocity with the square-root of the (upstream) distance along the surface. In fact, the present analysis strongly suggests that the position of P_D adjusts in a subtle manner, such that the solution of the BL equations terminates in form of a Goldstein singularity that (i) takes place at P_D and, simultaneously, (ii) is vanishingly weak, even though the BV singularity is found to be of finite strength.

2 Problem formulation

2.1 Governing equations

Let $\mathbf{x} = \mathbf{e}_x x + \mathbf{e}_y y + \mathbf{e}_z z$, $\mathbf{u} = \mathbf{e}_x u + \mathbf{e}_y v + \mathbf{e}_z w$, t, and p denote, respectively, the position and the velocity vector, the time, and the pressure, non-dimensional with the reference quantities, respectively, $\tilde{L}$, $\tilde{U}$, $\tilde{L}/\tilde{U}$, and $\tilde{\rho}\tilde{U}^2$, introduced in Sect. 1. Here, $\mathbf{x}$ and $\mathbf{u}$ are expressed using natural coordinates, where the unit vectors $\mathbf{e}_x$, $\mathbf{e}_y$, and $\mathbf{e}_z$ point in the directions along and normal to the body contour, which is given by $y = 0$, and perpendicular to the (x, y)-plane, respectively. The origin $\mathbf{x} = \mathbf{0}$ is taken to coincide with the front stagnation point P_F, see Fig. 1a. The Navier–Stokes equations for incompressible flow, subject to the usual no-slip condition holding at the body surface, then read

$$\nabla \cdot \mathbf{u} = 0, \tag{2.1}$$

$$\partial \mathbf{u}/\partial t + \mathbf{u} \cdot \nabla \mathbf{u} = -\nabla p + Re^{-1} \nabla^2 \mathbf{u}, \tag{2.2}$$

$$\mathbf{u}|_{y=0} = \mathbf{0}. \tag{2.3}$$

Equations (2) are supplemented with the requirement $|\mathbf{u}| \to 1$ as $y \to \infty$ for unperturbed parallel incident flow, see Fig. 1a. By adopting the curvilinear coordinate system introduced above, the gradient and the Laplacian are represented by $\nabla = \mathbf{e}_x\, h^{-1}\partial/\partial x + \mathbf{e}_y\, \partial/\partial y + \mathbf{e}_z\, \partial/\partial z$ and $\nabla^2 = h^{-1}[(\partial/\partial x)\,(h^{-1}\,\partial/\partial x) + (\partial/\partial y)\,(h\,\partial/\partial y)] + \partial^2/\partial z^2$, respectively. Herein $h := 1 + \varkappa(x)\, y$, where $\varkappa(x)$ denotes the surface curvature, which is assumed to be a quantity of $O(1)$ in general (and positive for a convex surface contour, as shown in Fig. 1a).

According to a well-known result of ergod theory, for a nominally stationary flow usual Reynolds-averaging of any (tensorial) flow quantity, in the following symbolized by $\mathbf{Q}$, is equivalent to time-averaging. Hence, we introduce the common Reynolds decomposition of $\mathbf{Q}$ into its time-mean value $\overline{\mathbf{Q}}$ and the statistically fluctuating contribution $\mathbf{Q}'$, by virtue of

$$\mathbf{Q}(\mathbf{x}, t; Re) = \overline{\mathbf{Q}}(x, y; Re) + \mathbf{Q}'(\mathbf{x}, t; Re), \tag{3.1}$$

$$\overline{\mathbf{Q}} := \lim_{\tau\to\infty} \frac{1}{\tau} \int_{-\tau/2}^{\tau/2} \mathbf{Q}(\mathbf{x}, t + \theta; Re)\, \mathrm{d}\theta. \tag{3.2}$$

Note that in the process of Reynolds-averaging, Eq. (3.2), the limit $\tau \to \infty$ is evaluated for *finite* values of Re. The accordingly averaged continuity equation (2.1) then is conveniently satisfied by introducing a stream function ψ such that $\partial\psi/\partial y = \overline{u}$, $\partial\psi/\partial x = -h\overline{v}$. In turn, averaging of the momentum equation (2.2) yields the well-known Reynolds equations for a nominally two-dimensional flow, [11] (p. 81),

$$h\left[\frac{\partial\psi}{\partial y}\frac{\partial}{\partial x} - \frac{\partial\psi}{\partial x}\frac{\partial}{\partial y}\right]\frac{\partial\psi}{\partial y} - \varkappa\frac{\partial\psi}{\partial x}\frac{\partial\psi}{\partial y} = -h\frac{\partial p}{\partial x} - h\frac{\partial\overline{u'^2}}{\partial x} - \frac{\partial\, h^2\,\overline{u'v'}}{\partial y} + \frac{h^2}{Re}\frac{\partial\,\nabla^2\psi}{\partial y}, \tag{4.1}$$

$$\left[\frac{\partial\psi}{\partial x}\frac{\partial}{\partial y} - \frac{\partial\psi}{\partial y}\frac{\partial}{\partial x}\right]\left[\frac{1}{h}\frac{\partial\psi}{\partial x}\right] - \varkappa\left[\frac{\partial\psi}{\partial y}\right]^2 = -h\frac{\partial p}{\partial y} - \frac{\partial\, h\overline{v'^2}}{\partial y} - \frac{\partial\overline{u'v'}}{\partial x} + \varkappa\,\overline{u'^2} - \frac{1}{Re}\frac{\partial\,\nabla^2\psi}{\partial x}. \tag{4.2}$$

It is of advantage to consider also the scalar transport equation for the time-mean value of the specific turbulent kinetic energy given by $q^2 := \mathbf{u}'\cdot\mathbf{u}'/2 \equiv (u'^2 + v'^2 + w'^2)/2$. In combination with the equations of motion (2) and (4), this equation conveniently serves to deduce the basic asymptotic scaling properties of the turbulent flow. Written in coordinate-free form,

$$\overline{\mathbf{u}} \cdot \nabla\,\overline{q^2} + \nabla \cdot \overline{(q^2 + p')\,\mathbf{u}'} - Re^{-1}\,\nabla^2\,\overline{q^2} + \varepsilon_p = P, \quad \varepsilon_p := Re^{-1}\,\overline{\nabla\mathbf{u}' : \nabla\mathbf{u}'}, \quad P := -\overline{\mathbf{u}'\mathbf{u}'} : \nabla\,\overline{\mathbf{u}}, \tag{5}$$

it results from Reynolds-averaging the inner product of $\mathbf{u}'$ with Eq. (2.2) by substituting Eq. (2.1). The positive definite quadratic form ε_p and the quantity P are usually referred to as turbulent (pseudo-)dissipation and turbulent production, respectively, [11] (p. 503 ff.).

2.2 Turbulent fluctuating motion

For what follows, we tacitly assume that in the limit (1) the turbulent velocity fluctuations u' and v' at a given point (x, y) are of the same order of magnitude, in general. Accordingly, their correlations $\overline{u'^2}$, $\overline{u'v'}$, $\overline{v'^2}$ are equally scaled (common hypothesis of locally isotropic turbulence). Also, let λ, Λ, and λ^+ denote characteristic values for the shortest spatial scales associated with the limit (1), non-dimensional with $\tilde{L}$, apparent in the fluctuating motion in, respectively, the external flow, the BL, and in the viscous wall layer located at the base of the latter. As a basic property of the fluctuating motion, here we only note that $\lambda \ll 1$.

3 Global asymptotic picture of the flow

We first focus on the intensity of the turbulent fluctuations by adopting a length scale comparable with the body dimensions, i.e. where x, y are quantities of $O(1)$. Then the quadratic form ε_p is asymptotically of $O(1)$ or smaller, as are the remaining contributions to Eq. (5). Following the arguments outlined in [7], it is very likely that λ is not asymptotically smaller than of $O(Re^{-1/2})$. In turn, the viscous term in the equations of motion (2) is seen to be negligibly small in the limit (1). In the region of the external or bulk flow, namely, outside the attached BL, the separated shear layer and the recirculating or wake flow region behind the body, respectively, see Fig. 1a, both $\mathbf{u}$ and p are of $O(1)$. Initially, let us also regard $|\mathbf{u}'|$ and p' as quantities of $O(1)$ there. By introducing appropriate small scales $(\mathbf{x}', t') = (\mathbf{x}, t)/\lambda$ and expanding $(\mathbf{u}, p) \sim (\mathbf{u}_0, p_0) + \cdots$, in this situation the Navier–Stokes equations (2.1) and (2.2) reduce to the Euler equations,

$$\nabla' \cdot \mathbf{u}_0 = 0, \quad \partial \mathbf{u}_0/\partial t' + \mathbf{u}_0 \cdot \nabla' \mathbf{u}_0 = -\nabla' p_0. \tag{6}$$

Herein, ∇' denotes the gradient with respect to $\mathbf{x}'$.

Let $\boldsymbol{\omega}$ denote the vorticity, $\boldsymbol{\omega} := \nabla \times \mathbf{u}$. Using standard algebra yields the scalar identity

$$\overline{\boldsymbol{\omega} : \boldsymbol{\omega}} \equiv \overline{\nabla \mathbf{u} : \nabla \mathbf{u}} - \nabla \cdot [\nabla \cdot (\overline{\mathbf{u} \cdot\cdot \mathbf{u}})]. \tag{7}$$

The specific form of the last term in Eq. (7) follows from substitution of the continuity equation (2.1). That term must be considered to be of $O(1)$ in general, according to Eqs. (3), whereas the above considerations here indicate that $\overline{\nabla \mathbf{u} : \nabla \mathbf{u}} \sim \overline{\nabla' \mathbf{u}_0' : \nabla' \mathbf{u}_0'} = O(\lambda^{-2})$. Therefore, this term provides the predominant contribution to the identity given in Eq. (7). On the other hand, as the oncoming bulk flow is assumed to be uniform, the property $\nabla \times \mathbf{u}_0 \equiv \mathbf{0}$ can be derived from Eqs. (6), indicating an irrotational flow. From Eq. (7) then follows that $\nabla' \mathbf{u}_0$ and, in turn, $\nabla' \mathbf{u}_0'$ vanishes, too. However, the latter result apparently contradicts the initial assumption that $|\mathbf{u}'| = O(1)$. Hence, we infer that in the external-flow region both the turbulent fluctuations and their correlations are small, rather than of $O(1)$. Since any effects of free-stream turbulence are disregarded there, the relatively weak fluctuations in the bulk flow are primarily caused by the much higher turbulence intensities in the attached BL and the separated shear layer, associated with highly concentrated vorticity there. Since these regions are relatively slender, the turbulence intensities there are still small compared to $O(1)$, which suggests that in the wake flow region, which exhibits relatively slow motion, they are of the same magnitude at the most. Let the small parameter α formally measure the magnitude of the components of the Reynolds stress tensor given by $-\overline{\mathbf{u}'\mathbf{u}'}$, without specifying any dependence of α on Re. We then arrive at the conclusion that, in the double limit $\alpha \to 0$ and $Re \to \infty$, the quantities $\mathbf{u}$ and p are (i) given by their time-mean values of $O(1)$ to leading order in the external-flow region, and (ii) are asymptotically small in the wake flow region.

The above considerations give rise to the following important result: in the region where x, y are of $O(1)$ Eqs. (4) reduce to the Euler equations to leading order, so that the bulk flow is to be sought in the class of steady irrotational flows with free streamlines. These detach from the body surface at the point P_D, indicated by $x = x_D$, and confine an (open, as in the case sketched in Fig. 1a, or closed) stagnant-flow region. Therefore, we anticipate the outer expansion

$$[p, \psi] \sim [p_0, \psi_0](x, y; k) + \cdots, \quad \nabla^2 \psi_0 = 0. \tag{8}$$

Here, the leading-order potential-flow solution is uniquely determined by the non-negative so-called BV parameter k, [2,14]. Accordingly, the streamwise gradient of the surface pressure is given by

$$(\partial p_0/\partial x)(x, 0; k) = -u_e \, \mathrm{d}u_e/\mathrm{d}x, \quad u_e(x; k) = (\partial \psi_0/\partial y)(x, 0; k). \tag{9}$$

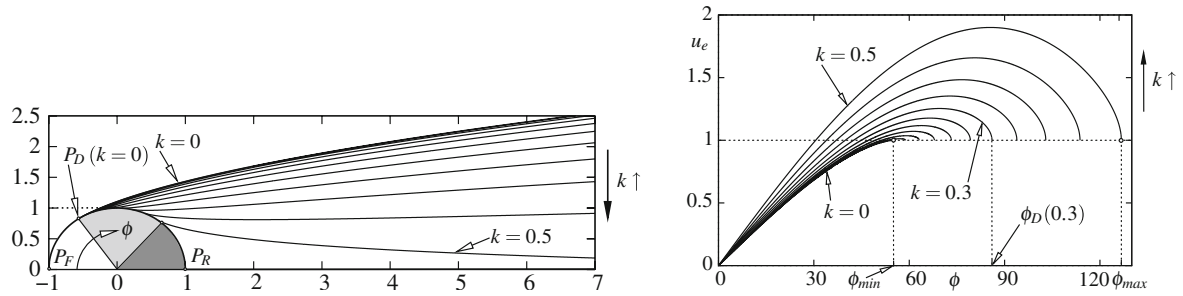

Fig. 2 Kirchhoff flow around a circular cylinder for discrete values $k = i \times 0.05$, $i = 0, 1, \ldots, 10$; **a** separating streamlines (figures on axes measure horizontal and vertical distance from centre in multiples of unit radius), **b** distribution $u_e(x; k)$ over arc angle ϕ [°], terminating in the singular manner given by Eq. (10.2) at $x = x_D(k)$, $\phi = \phi_D(k)$ (for example, $\phi_D(0.3) \doteq 86° 1' 54''$)

It is important for the subsequent analysis (see Subsect 5.3) that near the front stagnation point P_F the surface slip velocity $u_e(x)$ varies as

$$u_e(x; k) \sim b(k)\, x + O(x^2), \quad b(k) > 0, \quad x \to 0_+. \tag{10.1}$$

Moreover, it is well-known that $u_e(x; k)$ exhibits a square-root singularity immediately upstream of P_D, namely, the BV singularity already mentioned in Sect. 1, [2,15],

$$u_e(x; k)/u_e(x_D(k); k) \sim 1 + 2k(-s)^{1/2} + 10\,k^2(-s)/3 + O[(-s)^{3/2}], \quad s = x - x_D \to 0_-. \tag{10.2}$$

In the case $k = 0$, relevant for laminar separation, see Sect. 1, the second-order term in this expansion cancels out, such that $\partial p_0/\partial x$ is bounded at $x = 0$.

Without going into the technical details, we note that the Kirchhoff-type potential-flow problem for the canonical case of a circular cylinder in uniform cross stream, as referred to in Fig. 1a, has been solved numerically by employing the particular methods of conformal mapping elucidated in [2]. The solutions are displayed in Fig. 2. Let $\phi = 180\,x/\pi$ denote the arc angle measured from P_F. One then obtains $\phi = \phi_{\min} \doteq 55° 02' 30''$ for $k = 0$, cf. [2]. In general, for a convex surface contour the BV parameter k increases for increasing values $x = x_D(k)$, $\phi = \phi_D(k)$, characterizing the position of the point P_D. Also, in the case of a body shape which is symmetric with respect to the free-stream flow direction, the free streamlines have the form of a parabola sufficiently far downstream of the body under consideration and, therefore, confine an infinitely large dead-water zone. Specifically, in the canonical case depicted here, the inflection point of the free streamlines is shifted to infinity as $k \to k_{\max} \doteq 0.49079$, so that they meet asymptotically at infinity for $k = k_{\max}$ and $\phi = \phi_{\max} \doteq 126° 43' 32''$.

For geometrical reasons, $k \geq 0$. Also, $k \leq k_{\max}$ if the value of p_0 in P_D, equal to that and in the dead-water region, say, $p_{0,D}$, is that at infinity, say, $p_{0,\infty}$. For $k > k_{\max}$ the quantity of $p_{0,D}$ enters the problem as a further parameter, and the cusp-shaped stagnant-flow region has finite extent, cf. [13]. Here we only note that the strictly attached potential flow considered in [6] then is seen as the limit of a class of flows showing an increase of $p_{0,D}$ from $p_{0,\infty}$ up to the value of the pressure at the front and rear stagnation points P_F and P_R, respectively. Using Bernoulli's law, one finds that the latter is given by $p_{0,\infty} + 1/2$. Therefore, we expect that P_D approaches P_R when $k \to \infty$. In the following, we tacitly restrict the analysis to flows exhibiting an open cavity. Both regions are indicated by the light- and dark-shaded sectors in Fig. 2a.

4 Boundary layer exhibiting partially developed turbulence

4.1 Boundary layer approximation

We now assume "moderate" levels of turbulence intensities, so that the flow close to the surface is correctly described within the well-known framework of laminar BL theory. This is expressed by means of the appropriate inner expansion

$$\left[\psi,\ -\overline{u'v'}\right] \sim Re^{-1/2}\,\{[\Psi,\ T\mathscr{R}](x, Y; k, T) + \cdots\}, \quad Y = Re^{1/2}\,y. \tag{11}$$

The "strength" of the turbulent motion within the BL is accounted for by the (non-negative) turbulence intensity gauge factor T, mentioned in Sect. 1. In the most general case, this quantity is assumed to be of $O(1)$; thus, dots in Eqs. (8) and (11) stand for $O(Re^{-1/2})$. Stated equivalently, the root-mean-square values $(\overline{u'^2})^{1/2}$, $(\overline{v'^2})^{1/2}$ are taken to be of $O(\alpha^{1/2})$, where again a parameter,

$$\alpha := TRe^{-1/2}, \tag{12}$$

is adopted as a measure for the magnitude of the Reynolds stresses.

In combination with Eq. (9), the expansions (8) and (11) give rise to the laminar-type BL approximation of the streamwise momentum equation (4.1), having the form

$$\frac{\partial\Psi}{\partial Y}\frac{\partial^2\Psi}{\partial Y\partial x} - \frac{\partial\Psi}{\partial x}\frac{\partial^2\Psi}{\partial Y^2} = u_e\frac{\mathrm{d}u_e}{\mathrm{d}x} + T\frac{\partial\mathscr{R}}{\partial Y} + \frac{\partial^3\Psi}{\partial Y^3}. \tag{13.1}$$

Equation (13.1) is subject to the no-slip condition (2.3),

$$Y = 0: \quad \mathscr{R} = \Psi = \partial\Psi/\partial Y = 0. \tag{13.2}$$

In addition, matching with the external potential bulk flow requires the asymptotic behavior

$$Y \to \infty: \quad \mathscr{R} \to 0, \quad \partial\Psi/\partial Y \to u_e(x;k). \tag{13.3}$$

The purely laminar flow description is recovered in the case of a trivial solution for the Reynolds stress of the mixed laminar-turbulent BL problem posed by Eqs. (13), i.e. for $T\mathscr{R} \equiv 0$. However, in the subsequent analysis we seek solutions for non-trivial values of $T\mathscr{R}$, in general.

Equations (13) have to be be supplemented with initial conditions that adequately reflect the flow close to the (front) stagnation point $x = y = 0$, where u_e grows linearly with x according to Eq. (10.1). Furthermore, one infers from the hypothesis of local isotropy, stated in Subsect. 2.2, that $\mathscr{R}$ varies proportional to u_e^2. Both these issues are conveniently accommodated by applying the following transformation:

$$[\Psi,\, \mathscr{R}] = [u_e\,\Delta f,\, u_e^2\, r](x,\eta;k,T), \quad \Delta(x;k) = \frac{1}{u_e}\left(2\int_0^x u_e(\xi;k)\,\mathrm{d}\xi\right)^{1/2}, \quad \eta = \frac{Y}{\Delta}. \tag{14.1}$$

Then the BL problem (13) is rewritten as

$$\Delta^2\frac{\mathrm{d}u_e}{\mathrm{d}x}(f'^2 - 1) - ff'' + u_e\,\Delta^2\left(f'\frac{\partial f'}{\partial x} - \frac{\partial f}{\partial x}f''\right) = u_e\,\Delta\,Tr' + f''', \tag{14.2}$$

$$\eta = 0: \quad r = f = f' = 0, \quad \eta \to \infty: \quad r \to 0, \quad f' \to 1. \tag{14.3}$$

Herein the primes denote derivatives with respect to η. For a given distribution $u_e(x;k)$ satisfying the relationship (10.1), the specific choice of the scaling function $\Delta(x;k,T)$ in Eq. (14.1) results in a smooth approach for $x \to 0_+$ of Δ, r, and f towards the limits $\Delta(0;k) = b^{-1/2}$, $r(0,\eta;k,T) = r_0(\eta) \not\equiv 0$ and the initial condition for f, respectively:

$$f(0,\eta;k,T) = f_0(\eta), \quad f_0'^2 - f_0\,f_0'' = 1 + f_0''', \quad f_0(0) = f_0'(0) = 0, \quad f_0'(\infty) = 1. \tag{14.4}$$

That is, as $x \to 0$ the well-known laminar stagnation point solution, also referred to as Hiemenz flow, of the steady form of the Navier–Stokes equations (2) is recovered, cf. [11].

We finally stress that the solution of the initial-boundary value problem (14), where the imposed external streamwise velocity $u_e(x;k)$ satisfies Eqs. (10.1) and (10.2), is uniquely determined by the values of the two parameters k and T, respectively: the first one reflects the choice of the specific member of the class of Kirchhoff flows, while the second characterizes the magnitude of the Reynolds stress term entering Eq. (14.2). Amongst others (and as already mentioned in the Sect. 1), we will demonstrate numerically in Sect. 6.2 that both k and T can be chosen such that the behavior of the stream function f near $x = x_D$ accounts for the BV singularity, expressed in Eq. (10.2), in a way that allows to establish a local theory of separation.

4.2 Sublayer due to turbulence intensities

According to the definition of Λ given in Subsect. 2.2, its magnitude asymptotically does not exceed that of the BL thickness, which is of $O(Re^{-1/2})$. Inspection of the governing equations (2) then shows that $\mathbf{u}'$ and p' satisfy the Euler equations to leading order. Furthermore, it is demonstrated in [7] that $p' = O(q^2)$, where $q^2 \equiv |\mathbf{u}'|^2 = O(\alpha)$, by virtue of Eq. (12). In turn, for $Y = O(1)$ the least-degenerate BL approximation of Eq. (5) is readily found to be given by the balance between turbulent (pseudo-)dissipation and production,

$$\varepsilon_p \sim P, \quad P \sim T\mathscr{R}\,\partial^2\Psi/\partial Y^2 = O(T). \tag{15}$$

Equation (15) states that $\varepsilon_p = O(T)$ (remember that T is taken as a quantity of $O(1)$, in general). On the other hand, one infers from the definition of ε_p given in Eq. (5) that ε_p is asymptotically not larger than of $O\big(Re^{-1}\,\overline{q^2}/\Lambda^2\big)$. From these order-of-magnitude estimates we deduce that the reference length Λ typical for the most rapid spatial variation of the turbulent motion is presumably of $O(Re^{-3/4})$. Remarkably, its magnitude is comparable to the well-known (non-dimensional) Kolmogorov length that is of $O\big({\varepsilon_p}^{-1/4}\,Re^{-3/4}\big)$ by definition.

Due to the fact that Λ is asymptotically smaller than the BL thickness, in principal (but for $T > 0$ only) a further layer adjacent to the surface—not revealed by the Reynolds equations (4)—having a thickness of $O(\Lambda)$ has to be considered. Let this sublayer be described in terms of a coordinate $\hat{y}$ by setting

$$\hat{y} = y/\Lambda, \quad \Lambda = Re^{-3/4}. \tag{16}$$

For $\hat{y} = O(1)$ the leading-order form of Eq. (5) is seen to include the balance

$$\varepsilon_p \sim Re^{-1}\,\partial^2\overline{q^2}/\partial y^2 \tag{17}$$

in general, as a consequence of the no-slip condition Eq. (2.3). One also infers from Eq. (5) that $P \sim -\overline{u'v'}\partial\overline{u}/\partial y$ there, which asymptotically cannot be larger than ε_p. Hence, it follows from substituting Eq. (16) into Eq. (5) that the magnitude of $\overline{u}$ then does not exceed $O(Re^{-1/4})$. Moreover, we assume that $\overline{u'v'} = o(\overline{u})$ for $\hat{y} = O(1)$, as the remaining possibility $\overline{u'v'} = O(\overline{u})$ refers to the case of a fully developed turbulent BL, associated with the limit $T \to \infty$, which is addressed separately in Subsect. 5.1. The convective terms in Eqs. (4.2) appear to be negligibly small in the sublayer; the least-degenerate approximation of Eq. (4.1) then reads

$$\partial^2\overline{u}/\partial y^2 - \partial\overline{u'v'}/\partial y \sim \partial p_0/\partial x, \quad \partial p_0/\partial x \sim -u_e\,\mathrm{d}u_e/\mathrm{d}x = O(1). \tag{18}$$

By considering the BL equation (13.1), matching of $\overline{u}$ in the main layer where $Y = O(1)$ and in the sublayer then shows that in the latter $\overline{u} \sim Re^{-1/4}\,\hat{y}\,(\partial^2\Psi/\partial Y^2)_{Y=0}$. Herein the strictly positive coefficient $(\partial^2\Psi/\partial Y^2)_{Y=0}$ varies with x as part of the solution of Eq. (13.1).

In order to estimate the magnitude of the turbulent fluctuations, we also consider the most general least-degenerate form of the momentum equation (2.2) for $\hat{y} = O(1)$,

$$\partial\mathbf{u}'/\partial t + \overline{u}\,\partial\mathbf{u}'/\partial x \sim -\nabla p' + Re^{-1}\,\nabla^2\,\mathbf{u}'. \tag{19}$$

In this relationship, it is assumed that all components of ∇ are of $O(1/\Lambda)$, and the predominating time-mean quantities have been eliminated by using Eq. (18) and taking into account the aforementioned order-of-magnitude estimates. In Eq. (19) the second term on the left side and the viscous term are seen to be of $O(|\mathbf{u}'|\,Re^{1/2})$. Matching of $\mathbf{u}'$ and p' in the main and the sublayer shows that there is no asymptotically larger term present; otherwise, in the dominant balance $\partial\mathbf{u}'/\partial t \sim -\nabla p'$ the growth of, respectively, p' and the components of $\mathbf{u}'$ for $\hat{y} \to \infty$ would exhibit the identical dependence on $\hat{y}$, which in turn leads to the contradiction $p' = O(\overline{u}\,|\mathbf{u}'|)$ for $\hat{y} = O(1)$. In contrast, the second term in Eq. (19) shows the fastest growth for $\hat{y} \to \infty$ due to the aforementioned linear variation of $\overline{u}$ with $\hat{y}$. Thus, it has to be considered as negligibly small, which is only possible if our original assumption regarding the spatial gradients is relaxed by requiring that $\partial/\partial x = o(1/\Lambda)$. On this condition the leading-order approximation of the continuity equation (2.1) reads $\partial v'/\partial y \sim \partial w'/\partial z$. However, this most likely (albeit it is not demonstrated rigorously here) contradicts the requirement of identical growth rates of both v' and w' for $\hat{y} \to \infty$ due to the basic assumption of local isotropy, see Subsect. 2.2. The only possibility to surmount that disagreement in a self-consistent manner is to abandon that original assumption here by postulating a "degenerate" sublayer where $\partial/\partial z = o(1/\Lambda)$ also and, in turn, $|v'| \ll |u'|$, $|v'| \ll |w'|$. Then the x-component of Eq. (2.2) reduces to $\partial u'/\partial t \sim Re^{-1}\,\partial^2 u'/\partial y^2$. By

adopting the argument used in connection with the continuity equation, one finds that u' exhibits an unbounded growth for $\hat{y} \to \infty$, required by matching, only if the time-derivative can be neglected in this relationship. Finally, the no-slip condition (2.3) implies the expansions

$$[u', w'] \sim (T/Re)^{1/2}\, \hat{y}\, [U_0', W_0'](x, z; Re) + \cdots, \quad v' = T^{1/2} Re^{-3/4}\, \hat{y}^2\, V_0'(x, z; Re) + \cdots, \tag{20}$$

holding for $\hat{y} = O(1)$, where U_0', V_0' and W_0' are quantities of $O(1)$. To leading order, the continuity equation here reduces to the compatibility condition $\partial U_0'/\partial x + \partial W_0'/\partial z \sim -2\, V_0'$, whereas in Eq. (5) all terms are present apart from the first (convective) contribution. In fact, the originally assumed balance given by Eq. (17) is satisfied identically as both terms therein asymptotically equal $\alpha(U_0'^2 + W_0'^2)$. Accordingly, the two-term expansion for $\overline{u}$ simply follows from expanding the solution of Eqs. (13.1) and (13.2) for $Y \to 0$,

$$\overline{u} \sim Re^{-1/4}\, \hat{y}\, (\partial^2 \Psi/\partial Y^2)_{Y=0} - Re^{-1/2}\, \hat{y}^2\, (u_e\, \mathrm{d}u_e/\mathrm{d}x)/2 + \cdots. \tag{21}$$

We conclude from the above analysis that the sublayer behaves purely passive as the boundary conditions given by Eqs. (13.2) and (14.3) remain valid, even though they have to be interpreted correctly as matching conditions for $Y \to 0$ and $\eta \to 0$, respectively. However, in view of Eq. (20) they have to be restated more accurately in the form

$$Y \to 0: \quad \mathscr{R} = O(Y^3), \quad \eta \to 0: \quad r = O(\eta^3). \tag{22}$$

This result provides an important restriction on the formulation of an asymptotically correct Reynolds stress closure.

5 Fully developed turbulent boundary layer

The description of a fully developed turbulent (attached) BL is contained in the present approach by considering an (a priori unknown) appropriate double limit process $T \to \infty, Re \to \infty$, such that in Eq. (13.1) the molecular shear stress term, $\partial^2 \Psi/\partial Y^2$, becomes negligibly small compared to its turbulent counterpart, $T\mathscr{R}$, across the main portion of the BL. As a consequence of the no-slip condition (2.3), then in the so-called (viscous) wall layer located at the base of the main region of the fully turbulent BL the respective shear stress contributions $Re^{-1}\, \partial \overline{u}/\partial y$ and $-\overline{u'v'}$ in the momentum equation (4.1) are of the same order of magnitude.

In the light of the further analysis, we restrict the subsequent derivation of the essential properties of a turbulent BL to the so-called classical case of a two-tiered BL, describing firmly attached flow only. Formally, this is conveniently defined by two independent assumptions:

(A) In the viscous wall layer the (imposed) pressure gradient (which is of $O(1)$, in general) does not enter the leading-order balance of the momentum equation (4.1) in the limit (1);
(B) the outer fully turbulent main region can be directly matched with the viscous wall layer.

5.1 Viscous wall layer

Referring to Subsect. 2.2, that wall layer emerges where $y = O(\lambda^+)$. According to the rationale proposing the sublayer considered in Subsect. 4.2, here $\lambda^+ \ll 1$ measures the spatial scale typical for the turbulent dynamics in the region on its top in the limit (1). Then the balance expressed by Eq. (17) is met again. Herein ε_p is seen to predominate in the limit $y/\lambda^+ \to \infty$, so that further terms in Eq. (5) contribute in leading order to its least-degenerate form for $y = O(\lambda^+)$, hence given by

$$\partial\, \overline{(q^2 + p')v'}/\partial y - Re^{-1}\, \partial^2 \overline{q^2}/\partial y^2 + \varepsilon_p \sim P, \quad P \sim -\overline{u'v'}\, \partial \overline{u}/\partial y. \tag{23}$$

From the expression for P here it follows that $P = O(\overline{u}\, \overline{u'v'}/\lambda^+)$. We eliminate the Reynolds stress from this relationship by considering the presumed balance between the shear stress components, predicting that $\overline{u'v'} = O[\overline{u}/(\lambda^+ Re)]$, which yields $P = O(Re^{-1}\, \overline{u}^2/\lambda^{+2})$. Again, by adopting the assumption of locally isotropic turbulence, see Subsect. 2.2, we follow the arguments put forward in Subsect. 4.2: since P cannot be asymptotically larger than the quantity ε_p, the fundamental estimate $\varepsilon_p = O\left(Re^{-1}\, |\mathbf{u}'|^2/\lambda^{+2}\right)$ then immediately suggests that the magnitude of $\partial \overline{u}/\partial y$ does not exceed that of $\partial |\mathbf{u}'|/\partial y$.

At this point, these basic considerations, solely based on order-of-magnitude estimates of the time-mean quantities, strongly support a widely believed characteristic of the wall layer already proposed in Subsect. 4.2: namely, that $\overline{u}$ and all components of $\mathbf{u}'$ there are asymptotically of comparable magnitude. Stated equivalently, both the Navier–Stokes equations (2) and Eq. (23) are fully recovered to leading order. As the shear stress contributions are of $O(\overline{u}^2)$, the so-called skin-friction velocity u_*, where u_*^2 equals the (local) wall shear stress, provides a proper choice for the reference velocity. We then conveniently set $\lambda^+ = 1/(u_* Re)$ (which is of $O[1/(\lambda^+ Re^{3/2}\varepsilon_p^{1/2})]$ and, therefore, also asymptotically comparable to the Kolmogorov length, cf. Subsect. 4.2). In turn, the conventional wall layer expansion is revealed,

$$\left[\overline{u}/u_*, -\overline{u'v'}/u_*^2\right] \sim [u_0^+, s_0^+](x, y^+) + \cdots, \quad u_* = [Re^{-1}(\partial u/\partial y)_{y=0}]^{1/2}, \quad y^+ = y\, u_* Re. \tag{24}$$

In the momentum equation (4.1) the convective terms are of $O(u_*^2)$. Hence, they are negligibly small compared to the shear stress gradients, which are both of $O(u_*^2/\lambda^+)$. Integration of this balance with respect to y^+ subject to the assumption (A) above gives

$$\partial u_0^+/\partial y^+ + s_0^+ = 1, \tag{25}$$

note that $P/(u_*^5 Re) \sim s_0^+ \partial u_0^+/\partial y^+$, balancing $\varepsilon_p/(u_*^5 Re) = O(1)$. Most important, due to the no-slip condition (2.3) the behavior of the Reynolds stress close to the wall discussed in Subsect. 4.2 and subsumed in Eq. (22) is met again in the form $s_0^+ = O(y^{+3})$ as $y^+ \to 0$. This behavior relies on the reasonable assumption that in this limit both u'/u_* and w'/u_* vary regularly, i.e. linearly, with y^+, giving $v'/u_* = O(y^{+2})$, by virtue of the continuity equation (2.1).

Considering the behavior far from the surface, the obvious requirement that the viscous term in Eq. (25) vanishes is accomplished by the celebrated logarithmic law of the wall,

$$s_0^+ \sim 1 - (\kappa\, y^+)^{-1} + \cdots, \quad y^+ \to \infty, \tag{26.1}$$

$$u_0^+ \sim \kappa^{-1} \ln y^+ + C^+ + \cdots, \quad \kappa \approx 0.384, \quad C^+ \approx 4.1, \quad y^+ \to \infty. \tag{26.2}$$

In Eq. (26.2) the values for the v. Kármán constant κ and the quantity C^+ refer to a perfectly smooth surface [9]. Most important, in recent studies it is pointed out how this commonly assumed behavior can remarkably be deduced from a rigorous investigation of the unsteady motion the viscous wall layer, see [9] and the references therein. Also, there it is found that u_0^+, s_0^+ are presumably representing "universal" functions, i.e. independent of x, even for $y^+ = O(1)$.

5.2 Outer small-defect layer

We now briefly recall the basic characteristics of the main portion of the BL, cf. [11]. At first we note the well-known property that, in striking contrast to the case presented in Sect. 4, a fully turbulent BL typically exhibits a relatively pronounced outer edge. Considering the time-averaged BL having a (local) thickness denoted by δ, here approximated by the curve $y = \delta$, separates the external from the strongly turbulent flow.

The aforementioned assumption (B) of a common overlap conjoining the main layer and the viscous wall layer allows for a match of these flow regions. The matching process based on the wall layer scalings and the behavior for $y^+ \to \infty$ expressed by Eqs. (24) and (26), respectively, then confirms the well-known observation that the streamwise velocity defect defined by $u_e - \overline{u}$ is of $O(u_*)$ across the outer main layer. The associated outer-layer expansions are given by

$$\left[\frac{u_e - \overline{u}}{u_*}, \frac{-\overline{u'v'}}{u_*^2}\right] \sim [h_1', s_1](x, \zeta) + O(\gamma), \quad \delta(x; Re) \sim \gamma\, \delta_1(x) + O(\gamma^2), \quad \zeta = \frac{y}{\delta}, \tag{27.1}$$

provided that the so-called skin-friction law determining the quantity γ in the limit $Re \to \infty$,

$$\gamma := u_*/u_e \sim \kappa\sigma\,[1 + 2\sigma \ln\sigma + O(\sigma)], \quad \sigma := 1/\ln Re, \tag{27.2}$$

holds. In Eq. (27.1) any further dependences, e.g. on the BV parameter k, are not indicated for the sake of simplicity. Furthermore, here and in the following derivatives with respect to ζ are denoted by primes also. Note that the imposed pressure gradient is cancelled by the leading-order convective term, cf. [8], and from

Eq. (27.2) the assumption (B) is found to be consistent with the assumption (A). In turn, the sublayer thickness λ^+ is seen to be of $O[1/(Re\ \ln Re)]$.

Substituting Eqs. (27) into the Reynolds equations (4) results in a leading-order equation exhibiting linearized convective terms. Integrating it with respect to ζ yields

$$u_e^2[\partial(u_e\,\delta_1)/\partial x]\,\zeta h_1' - \partial(u_e^3\delta_1\,h_1)/\partial x = u_e^3(s_1 - 1), \tag{28.1}$$

by taking into account Eqs. (26). That is, h_1, s_1 satisfy the matching and boundary conditions

$$\zeta \to 0: \quad h_1 \to 0, \quad h_1' \sim -\kappa^{-1}\ln\zeta + c_1(x), \quad s_1 \to 1, \quad \zeta = 1: \quad h_1' = s_1 = 0. \tag{28.2}$$

Here, the function $c_1(x)$ is part of the solution for $h_1(x,\zeta)$, and the conditions for $\zeta = 1$ reflect the behavior near the BL edge.

5.3 Gradual departure from Hiemenz flow

The analysis of Subsect. 4.1 indicates that, as a consequence of the behavior of u_e close to the front stagnation point, expressed through Eqs. (10.1) and (14.4), the convective terms still balance both the shear stress contributions in Eq. (14.2) in a small region where $x = O(1/T)$. In the following we focus on that flow regime, which accounts for the laminar-turbulent transition process as $T \to \infty$. Inspection of the momentum equations (4.2) shows that the BL approximation $\partial/\partial y \gg \partial/\partial x$ remains valid there if the parameter α introduced in Eq. (12) is considered to be small in the aforementioned double limit. In turn, the stagnating-flow limit, see Eq. (14.4), is assumed in a narrower region, where both x and y are of $O(Re^{-1/2})$. Furthermore, the BL approximation is assumed to hold also further downstream where $x = O(1)$. Therefore, we treat the flow within the framework of BL theory where $x = O(1/T)$ and then show by matching with the fully developed turbulent flow further downstream that indeed $\alpha \to 0$.

To this end, we introduce suitably rescaled variables, taken to be of $O(1)$, and expand f, r in terms of

$$[f, r] \sim [F, R](X, \eta) + \cdots, \quad \Delta \sim b^{-1/2} + \cdots, \quad X = b^{1/2}\,Tx, \tag{29.1}$$

in accordance with the behavior of u_e given in Eq. (10.1). To leading order, the BL equation (14.2) then is transformed into

$$F'^2 - FF'' + X(F'\,\partial F'/\partial X - F''\,\partial F/\partial X) = 1 + XR' + F'''. \tag{29.2}$$

This equation is subject to the boundary and initial conditions (14.3) and (14.4) where formally f and r have to be replaced by F and R, respectively.

5.3.1 Asymptotic form of the flow far downstream

A treatment of the problem of separation that is consistent with the global flow structure requires the knowledge of the asymptotic splitting of the oncoming BL sufficiently far upstream of P_D, where $x = O(1)$, see Fig. 1. In the case considered here, the attached BL originates from the region of laminar-turbulent transition where $X = O(1)$. Therefore, the picture of the fully turbulent flow has to be deduced from an investigation of the BL equation (29.2), by taking into account Eq. (29.1) and the boundary conditions given by Eq. (14.3), in the limit $X \to \infty$. We emphasize that the scalings expressed by Eqs. (24) and (29.1) are the only assumptions concerning the behavior of the Reynolds shear stress r adopted in the subsequent investigation, which provides the description of the downstream evolution of the BL flow in the region $X = O(1)$. Therefore, the analysis not only turns out to be largely independent of any turbulence closure but, most important, imposes a restriction on any asymptotically correct model for r that is consistent with the generation of the fully turbulent BL for $X \to \infty$.

Specifically, any correct closure has to predict the associated well-known focussing of the BL edge to a pronounced, i.e. for $X \to \infty$ asymptotically narrow zone, namely, the so-called viscous superlayer. As already mentioned in Subsect. 5.2, however, this flow region is disregarded in the following and the position of the "turbulent" BL edge emerging for $X \to \infty$ here is expressed in form of the line $Y \sim \Delta_T(X) \sim Re^{1/2}\delta$. Therefore, the quantity Δ_T characterizes the formation of the "turbulent" BL thickness and is determined in the course of the subsequent analysis. We now discuss the resulting asymptotic flow structure, sketched in Fig. 1.

In the expansions describing the flow in the main layer,

$$[F, R](X, \eta) \sim [H/\rho, S](X, \zeta) + \cdots, \quad \Delta/\Delta_T \sim \rho(X) + \cdots, \quad \zeta = \rho(X)\,\eta, \ \ X \to \infty, \tag{30.1}$$

the "turbulent" BL coordinate ζ is assumed to be of $O(1)$ and the gauge function $\rho(X)$ is not known in advance. In turn, the accordingly transformed Eq. (29.2) gives

$$H'^2 - \rho[\mathrm{d}(X/\rho)/\mathrm{d}X]\,HH'' + X(H'\,\partial H'/\partial X - H''\,\partial H/\partial X) \sim 1 + X\rho S' + \rho^2 H'''. \tag{30.2}$$

The requirement that the viscosity-induced shear rate $\rho^2 H''$ is insignificantly small compared to the Reynolds stress term $X\rho S$ in the limit $X \to \infty$ yields $X/\rho \to \infty$. Furthermore, the boundary conditions to be satisfied at the outer edge of the turbulent BL, here characterized by $\zeta = 1$, give $H'(X, 1) \to 1$ and $S(X, 1) \to 0$ as $X \to \infty$. The first of these relationships then indicates that the expansion

$$[H, S] \sim [H_0, S_0](\zeta) + [\gamma_H(X)\,H_1(\zeta),\ \gamma_S(X)\,S_1(\zeta)] + \cdots, \quad (\gamma_H, \gamma_S) \to (0, 0), \quad X \to \infty, \tag{31}$$

holds in the main layer where $\zeta = O(1)$ with the a priory unknown gauge functions $\gamma_H(X)$, $\gamma_S(X)$.

5.3.2 Case: large-defect flow

We first assume that $S_0 \not\equiv 0$ in Eq. (31). Then the streamwise velocity defect with respect to the external flow is given by $1 - H_0'$ and seen to be of $O(1)$. By substituting Eq. (31) into Eq. (30.2) one readily finds that

$$H_0'^2 - 2\,H_0\,H_0'' = 1 + S_0'/a, \quad H_0(0) = 0, \ \ H_0'(1) = 1, \ \ S_0(1) = 0. \tag{32}$$

Herein a is a (positive) constant of $O(1)$ such that $\rho \sim 1/(aX)$ or, by noticing Eq. (30.1),

$$\Delta_T \sim a\,b^{-1/2}\,X, \quad X \to \infty. \tag{33}$$

Then, as indicated by matching subject to Eqs. (11), (12), and (29.1), the thickness of the fully turbulent BL where $x = O(1)$ is of $O(\alpha)$. In the subsequent two paragraphs we outline in brief that Eq. (32) does not allow for any physically admissible solution H_0, S_0 that is consistent with the asymptotic splitting of the BL flow.

The obvious restrictions $0 \le H_0' \le 1$ and, in turn, $H_0'' \ge 0$ for $0 \le \zeta \le 1$ yield $H_0\,H_0'' \to 0$ as $\zeta \to 0$ and, as a result, $S_0'(0) \le 0$. From the last boundary condition in Eq. (32) then inevitably follows that $S_0(0) > 0$ (and, consequently, $H_0'(0) < 1$). Furthermore, inspection of Eq. (30.2) shows that for small values of ζ the convective and the pressure gradient terms are negligibly small compared to the Reynolds stress gradient. Thus, for $X \to \infty$ close to the surface a sublayer of a relative thickness, say, $\Delta^+(X)$ with $\Delta^+ \to 0$, emerges. That flow region is governed by the limiting forms

$$H \sim \gamma_H^+ \Delta^+ H^+(\zeta^+), \quad S \sim S_0(0)\,S^+(\zeta^+), \quad \zeta^+ = \zeta/\Delta^+ = O(1), \tag{34.1}$$

where an asymptotically correct choice for the gauge function γ_h^+ is provided by

$$\gamma_H^+ \sim a\,S_0(0)\,X^2\Delta^+. \tag{34.2}$$

Equations (30.2) and (34.1) then give rise to the leading-order balance

$$H^{+\prime\prime} + S^+ \sim 1, \tag{34.3}$$

here the primes denote derivatives with respect to the sublayer coordinate ζ^+. Equation (34.3) states that this sublayer is gradually transformed into the viscous wall layer, described in Subsect. 5.1, which takes place where $x = O(1)$, such that ζ^+ is replaced by y^+. Therefore, we expect a behavior of the form

$$H^{+\prime} \sim \kappa^{-1} \ln \zeta^+ + \cdots, \quad S^+ \sim 1 + \cdots, \quad \zeta^+ \to \infty. \tag{34.4}$$

That is, in an additional asymptotic flow region to be considered, located between that sublayer and the main region, Eq. (30.2) reduces to $S \sim S_0(0)$ in leading order. Matching with the adjacent layers then requires that any possibly admissible solution of Eq. (32) is characterized by $H_0'(0) > 0$, which expresses a finite slip velocity at the base of the outermost layer. In turn, it follows from Eq. (34.4) that $\gamma_H^+ \sim -\kappa\,H_0'(0)/\ln\Delta^+$, where $\Delta^+ \sim \kappa\,H_0'(0)/[2\,a\,S_0(0)\,X^2 \ln X]$, according to Eq. (34.2). On the other hand, by virtue of the scalings

provided by Eqs. (24) and (27.2), the thickness of the viscous wall layer asymptotically varies inversely proportional to $x\,\gamma\,Re$ as $x \to 0$. By using Eq. (12), from matching this expression with that for the sublayer thickness, given by $Re^{-1/2}\Delta_T\,\Delta^+$, one then finds that $T \ln T = O(\gamma\,Re^{1/2})$. This is included in the more precise relationship $T \ln^2 T = O(Re^{1/2})$ that follows from matching of both $\overline{u}$ and the shear stress $-\overline{u'v'}$ in the sublayer and the wall layer, which yields $\gamma \sim \gamma_H^+ = O(1/\ln T)$ and, see Eq. (12), $\alpha = \gamma^2\,[= O[1/(\ln Re)^2]]$, respectively. Finally, a "skin-friction law" of the form

$$\gamma \sim \kappa\, H_0'(0)\,\sigma[1 - \sigma \ln\sigma + O(\sigma \ln\sigma)], \tag{35}$$

akin to Eq. (27.2), but for $H_0'(0) < 1$, can be obtained. By considering the BL where $x = O(1)$, one derives an analogous result by matching the viscous wall layer and the middle layer that emanates from the aforementioned intermediate layer and exhibits a small streamwise velocity deficit of $O(\gamma)$ with respect to the slip velocity imposed by the outer layer (having itself a large velocity defect). We note that the here resulting three-tiered BL structure essentially corresponds to that proposed by Melnik [4].

According to the logarithmic variation of u with respect to y^+ in the overlap of the viscous wall layer and the region located on its top, epitomized in [9], the smallest spatial scales in y-direction apparent in these flow layers are given by the thicknesses of the latter, whereas those in x- and z-direction are regarded to be of $O(\lambda^+)$ in both layers, cf. Subsect. 5.1. Specifically, here $-\overline{u'v'} = O(\alpha)$ and, cf. Subsect. 2.2, $\mathbf{u}' = O(\alpha^{1/2})$ throughout the BL, but the smallest spatial scales (in all three directions) are of $O(Re^{-3/4})$ in the outer main layer, see the analysis of Sect. 3, but of $O(\lambda^+)$ in the middle layer. However, this behavior is apparently inconsistent with the existence of a common overlap of these flow regions with respect to matching of $\mathbf{u}'$.

5.3.3 Case: small-defect flow

As a consequence of this inconsistency, it is strongly supposed that the accelerating BL in a transitional state assumes a degenerate form, here expressed through $S_0 \equiv 0$, in the limit $X \to \infty$. From differentiating Eq. (32) one then readily verifies that it is correctly replaced by $H_0' = 1$, giving $H_0 = \zeta$, as the appropriate lowest-order reduction of Eq. (30.2). In this case, evidence for the choice $\gamma_S \to 0$ [tacitly adopted in Eq. (31)], in addition to the, for $S_0 \equiv 0$, also acceptable possibility $\gamma_S = O(1)$, is provided by the subsequent analysis. First, with respect to the expansion (31), we note that the expression $-\gamma_H H_1'$ is recognized as the asymptotic representation for $X \to \infty$ of the strictly positive relative streamwise velocity defect in the main layer, given by $1 - \overline{u}/u_e$. Hence, we stipulate $H_1' > 0$, $H_1 > 0$ there and $\gamma_H < 0$.

Considering the first-order perturbation of the thereby recovered inviscid (Euler flow) limit, see Eq. (31), the least-degenerate form of Eq. (30.2) in the limit $X \to \infty$ reads

$$\Omega_1 H_1' - \Omega_2\,\zeta\,H_1'' \sim X^2\rho\gamma_S\,S_1', \quad \Omega_1 := \mathrm{d}(X^2\gamma_H)/\mathrm{d}X, \quad \Omega_2 := X\rho\gamma_H[\mathrm{d}(X/\rho)/\mathrm{d}X]. \tag{36}$$

Again, herein the viscous shear stress term is discarded, by assuming

$$X\gamma_S/(\rho\gamma_H) \to -\infty, \quad X \to \infty. \tag{37}$$

Integrating Eq. (36) by parts with respect to ζ and subject to the apparent boundary conditions $H_1(0) = H_1'(1) = S_1(1) = 0$ then yields

$$(\Omega_1 + \Omega_2)\,H_1 - \Omega_2\,\zeta\,H_1' \sim X^2\rho\gamma_S[S_1 - S_1(0)], \quad \Omega_1 + \Omega_2 = (\rho/X)\,\mathrm{d}(X^3\gamma_H/\rho)/\mathrm{d}X. \tag{38}$$

By noting that $H_1(1) > 0$, evaluation of this relationship for $\zeta = 1$ shows that the term on the right-hand side enters its leading-order approximation. Then the main portion of the BL in the flow region where $x = O(1)$ is seen to be of small-defect type, analogous to that considered in Subsect. 5.2. Moreover, it is readily verified that the momentum equations (4.1) and (4.2) give rise to Eq. (28.1) in leading order as the expansions expressed by Eq. (27.1) are retained, where the three gauge functions u_*, u_*^2, and γ for $\overline{u}$, $-\overline{u'v'}$, and δ, respectively, are, in general, replaced by appropriate counterparts. Also, the boundary conditions in Eq. (28.2) hold necessarily, apart from the matching conditions for h_1' and s_1 for $\zeta \to 0$. Specifically, in the case of a more complex (i.e. three-tiered) turbulent BL structure, the latter is to be replaced by $s_1(x, 0) = 0$. Moreover, from Eqs. (10.1) and (28) and the repeated use of ζ in Eqs. (27.1) and (30.1) we infer that

$$[h_1, s_1](x, \zeta) \sim [H_1, S_1](\zeta) + O(x), \quad \delta_1 \sim \Delta_1 x + O(x^2), \quad x \to 0, \tag{39}$$

where Δ_1 is a positive constant. However, then also $s_1(0,0) > 0$, since all terms in Eq. (28.1) are seen to be of $O(x^3)$ as $x \to 0$ and $H_1(1) > 0$. In turn, $s_1 > 0$ for all $x \geq 0$. From the matching conditions provided by the analysis of the wall layer, see Eqs. (26), we then draw the important conclusion that there exists a common overlap with the small-defect (main) layer: that is, the BL at distances of $x = O(1)$ is of the classical small-defect type considered in Subsect 5.2. Finally, we conveniently set $S_1(0) = s_1(x,0) \equiv 1$, and the leading-order form of Eq. (38) reads

$$\zeta H_1' - 2 H_1 = 2 H_1(1)[S_1 - 1], \quad H_1(1) = 1/(4\Delta_1), \tag{40.1}$$

subject to the boundary conditions

$$\zeta = 0: \quad H_1(0) = 0, \quad H_1 \sim -\kappa^{-1} \ln \zeta + C_1, \quad S_1(0) = 1, \quad \zeta = 1: \quad H_1'(1) = S_1(1) = 0. \tag{40.2}$$

Note that the constant C_1 in Eq. (40.2) is to be determined from the solution for $H_1(\zeta)$.

We now envisage the gauge functions. Matching the thickness δ of the fully turbulent BL involves the gauge function $\rho(X)$, introduced in Eq. (30.1), in the form

$$\delta \sim Re^{-1/2} \Delta_T \sim (b\,Re)^{-1/2}/\rho. \tag{41}$$

Furthermore, since all terms in Eq. (38) are of equal magnitude, comparison with Eq. (40.1) yields

$$X^2 \rho \gamma_S \sim -2 H_1(1)\, \Omega_1, \quad \Omega_1 = \Omega_2 < 0 \tag{42}$$

(note that $\gamma_H < 0$). The first relationship in Eq. (42) is confirmed by considering Eq. (28.1) as the balance between the Reynolds stress gradient and the convective terms in the form $-\overline{u'v'}/\delta = O[\mathrm{d}(u_e^2 \gamma_H)/\mathrm{d}x]$. In agreement with the matching principle, this balance can be expanded when expressed in terms of X and evaluated for $T \to \infty$ with X kept fixed. In fact, by taking into account Eqs. (10.1), (11), (12), (41), the scalings given by Eqs. (14.1), (29.1), (30.1), and noting that $\partial/\partial x \sim T^{-1} \partial/\partial X$, it is rewritten as $X^2 \rho \gamma_S \propto -\Omega_1$ to leading order. Furthermore, integration of the latter equality in Eq. (42) can be carried out easily to give

$$X\rho = -\Gamma(X)/\gamma_H, \quad \ln \Gamma = o(\ln X), \quad X \to \infty, \tag{43}$$

by introducing a further (rather slowly varying positive) gauge function $\Gamma(X)$. The behavior of $\ln \Gamma$ in Eq. (43) follows from the estimate $1/\gamma_H = o(X^2)$, deduced from the expression for Ω_1 in Eq. (36). Then Eq. (43) gives $\rho \to 0$. Thus, the variation of δ_1 with x in Eq. (39) complies with the matching condition Eq. (41).

As the main layer analysis outlined so far is not rich enough to determine the gauge functions γ_H, γ_S, ρ, and, hence, the variation of T with Re, we next consider the sublayer close to the surface, where the viscous shear stress comes into play to leading order. That sublayer is gradually transformed into the viscous wall layer taking place where $x = O(1)$; see the above analysis for the (hypothetical) case of a large velocity defect. We introduce further gauge functions $\gamma_H^+(X)$, $\gamma_S^+(X)$ and conveniently describe that sublayer by adopting Eqs. (34). Therein we formally replace $S_0(0)$ by γ_S^+ and, hence, Eq. (34.2) in the now appropriate form

$$\gamma_H^+/\gamma_S^+ = X\Delta^+/\rho. \tag{44.1}$$

From $S_1(0) > 0$ and Eq. (34.4) one then infers

$$\gamma_H = -\gamma_H^+ \sim \kappa/\ln \Delta^+, \quad \gamma_S = \gamma_S^+. \tag{44.2}$$

As a first result, the aforementioned requirements $\Delta^+ \to 0$ and $\gamma_H < 0$ are seen to interdepend mutually, and the assumption stated by Eq. (37) is validated by inserting Eq. (44.1). We then advantageously eliminate γ_S and ρ by substituting Eqs. (44) and (43) into Eq. (42), giving $\Gamma^2 = 2 H_1(1)\, X \Delta^+ \gamma_H \Omega_1$. By logarithmizing this relationship, one suitably eliminates Δ^+ by means of Eq. (44.2). Taking into account Eqs. (36) and (43) and that $\ln(-\gamma_H) = o(1/\gamma_H)$, eliminating Δ^+ by means of Eq. (44.2) then leads to the least-degenerate form of the dependence of γ_H on X,

$$\kappa/\gamma_H + 2 \ln X \sim -\ln(1+\chi), \quad \chi := X(\mathrm{d}\gamma_H/\mathrm{d}X)/(2\gamma_H), \quad X \to \infty. \tag{45}$$

Herein χ is seen to be bounded, since $\gamma_H \to 0_-$ requires $\chi < 0$; otherwise, γ_H would exhibit super-exponential growth, which does not allow for a match. In turn, we arrive at the important results

$$\gamma_H = -\kappa/(2 \ln X), \quad \gamma_S = \gamma_H^2/(\Delta_1 \Gamma), \quad \rho = 2[\Gamma(X) \ln X]/(\kappa X), \quad \Delta^+ = \Delta_1 \rho^2, \quad X \to \infty. \tag{46}$$

The relationships for γ_S, ρ, Δ^+ in Eq. (46) are determined from evaluating Ω_1 in Eq. (36) and by adopting Eqs. (42), (43) and (44.1), where $H_1(1)$ is expressed in terms of Δ_1 by using Eq. (40).

Finally, matching the BL thickness according to Eq. (41) and the Reynolds stress provides two asymptotic relationships that can be cast into the single one

$$\Gamma(X)\,(\ln T)^2/[\alpha\, H_1(1)] \sim 2\ln Re\,\ln T \sim (\ln Re)^2, \quad X = O(T) \quad \Leftrightarrow \quad x = O(1). \tag{47.1}$$

By recalling that the turbulence intensity gauge factor $T = \alpha\, Re^{1/2}$, see Eq. (12), one then finds

$$\Gamma/\alpha \sim 4\, H_1(1) = 1/\Delta_1, \quad \ln\alpha = o(\ln Re). \tag{47.2}$$

Remarkably, the dependence of α on Re is governed by the specific form of the still unknown gauge function $\Gamma(X)$, introduced in Eq. (43). However, it is assumed to assure that $\alpha \to 0$ in the limit (1), in order to justify the BL approximation for $X = O(1)$, and, in turn, that $\gamma_H \sim -\gamma$ for $x = O(1)$. Simultaneously, Eq. (47.2) requires that $\Gamma \to 0$ as $X \to \infty$. For example, if $\Gamma = 4\, H_1(1)/(\ln X)^2$ then $\alpha \sim 1/(\ln T)^2 \sim 4/(\ln Re)^2$, such that $\gamma_S = \kappa^2/4$, see Eq. (46). However, it is very likely that an estimate for $\Gamma(X)$, which is more precise than that given in Eq. (43) and largely independent of a specific Reynolds stress closure, is found in the course of the analysis of the higher-order terms indicated by dots in Eq. (31) (and an investigation of the viscous superlayer), not considered here. Specifically, the expansions given in Eq. (27.1) are unaffected by eigensolutions, such that the remainder terms are correctly anticipated to be of $O(\gamma)$ and $O(\gamma^2)$, respectively, if

$$\Gamma(X) = -\gamma_H/\Delta_1 = \kappa/(2\,\Delta_1 \ln X), \quad \gamma_S = -\gamma_H \quad \Leftrightarrow \quad \alpha \sim \kappa/\ln Re \sim \gamma. \tag{47.3}$$

We note that the question whether there exists an uniquely determined distinguished limit $T \to \infty$ as $Re \to \infty$ is a topic of the current research.

5.4 Fully turbulent flow along body surface

Unfortunately, however, these considerations are apparently inconsistent with the here presumed scaling of the Reynolds shear stress, given by Eqs. (11) and (12), that underlies the specific form of the BL problem (13) obtained for $T \to \infty$: for $\alpha \ll 1$, the wall layer analysis presented in Subsect. 5.1 is expected to hold in slightly modified form, [6], as a novel velocity scale, say, u_T with $u_T = u_*/\alpha^{1/2}$ ($\gg u_*$), replaces u_* and, equivalently, $-\overline{u'v'} \sim \alpha u_T^2 s_0^+$. Accordingly, the stress balance then yields a wall layer thickness $\lambda^+ = 1/(u_T \alpha Re)$.

Most important, the main results of the theory, namely the from of the matching conditions (26), are still valid, such that the outer layer expansion (27.1) is replaced by

$$\left[\frac{u_e - \overline{u}}{u_T},\ \frac{-\overline{u'v'}}{\alpha u_T^2}\right] \sim [h_1', s_1](x,\zeta) + O(\gamma_T), \quad \frac{\delta(x;T,Re)}{\alpha} \sim \gamma_T \delta_1(x) + O(\gamma_T^2), \quad \zeta = \frac{y}{\delta}. \tag{48.1}$$

Herein, the quantity γ_T measuring the velocity defect is determined by the corresponding analogon to the skin-friction law (27.2). By making use of Eq. (12), one now obtains

$$\gamma_T := u_T/u_e \sim \kappa\sigma_T\,[1 - 2\sigma_T \ln\sigma_T + O(\sigma_T)], \quad \sigma_T := 1/(2\,\ln T). \tag{48.2}$$

In turn, Eqs. (28) are recovered. Also, these leading-order results for the outer layer can be readily derived from the BL equations (13), see [6], or, equivalently, (14.1)–(14.3).

For instance, the above description of the turbulent main layer is obtained by expanding Eqs. (13.1) and (13.3) for $\zeta = O(1)$, after inserting

$$Y = Re^{1/2}\gamma_T\,\delta_1\zeta, \quad \Psi \sim Re^{1/2}\gamma_T\,\delta_1 u_e(\zeta - \gamma\, h_1), \quad \mathscr{R} \sim Re^{1/2}\gamma_T^2\, u_e^2 s_1. \tag{49}$$

Accordingly, here the BL edge $y = \delta$ is represented in the form $Y \sim Re^{1/2}\gamma_T\delta_1$, cf. Eq. (41).

Matching the solutions for $X = O(1)$ and $x = O(1)$ then immediately gives $r = O(\gamma_T^2)$, see Eq. (14.1), and $\gamma_H \sim -\gamma_T$ for $x = O(1)$. The latter relationship again yields the in (48.2) anticipated result $\gamma_T \sim \kappa/(2\ln T)$, cf. [6], whereas the former removes the aforementioned uncertainty in the choice of $\Gamma(X)$ (quite naturally) as it requires

$$\Gamma = 1/\Delta_1, \quad \gamma_S = \gamma_H^2 \quad \Leftrightarrow \quad \alpha = o(1). \tag{50}$$

Finally, matching of the BL thickness δ, see Eqs. (48), with its expression given by Eqs. (41) and (43) is easily verified. Equation (50) provides the counterpart to the relationships (47) that fully complies with the large-T limit of, respectively, Eqs. (13) and (14).

As a result, we arrive at the remarkable – preliminary – conclusion that in the limit $T \to \infty$ a generalized form of the classical theory, subsumed in Subsects. 5.1 and 5.2, applies for $x = O(1)$. Then the magnitude of the velocity defect in the outer region is found to be of $O(1/\ln T)$ and reaches its theoretically possible minimum in the case of the classical flow description that refers to a fully developed turbulent BL. As already pointed out in [6], this limit is simply included by setting $\alpha = 1$, i.e. $T = Re^{1/2}$, giving $\gamma_T = \gamma$ (as $\sigma_T = \sigma$). However, since we require $\alpha \to 0$ as $Re \to \infty$, here the existence of this limiting solution is prohibited as a consequence of the specific the asymptotic properties of the flow near the front stagnation point. Therefore, we feel it is important to distinguish between the here used term "fully turbulent" and "fully developed turbulent", which originally refers to the classically scaled turbulent BL.

6 Numerical treatment of the boundary layer flow

6.1 Asymptotically correct Reynolds stress closure

In order to obtain numerical solutions of the BL problem posed by Eqs. (14) for various values of k and T, the Reynolds shear stress is conveniently modelled on the basis of the mixing length formulation, which is associated with the concept of a sharp BL edge $y = \delta$, cf. [11].

In the case $T \to \infty$ the solutions shall assume a behavior that is compatible with the asymptotic structure derived in Sect. 5. This is achieved if the mixing length, here denoted by ℓ, is taken as the product of the two "lengths" l, l^+ that account for the BL flow in the main and the sublayer, respectively,

$$r = [\ell/\hat{\rho}]^2 f''(x,\eta;k,T)^2, \quad \ell = l(\zeta)\, l^+(y^+), \tag{51.1}$$

$$\zeta = \hat{\rho}(x;k,T)\eta, \quad y^+ = T u_T \Delta\eta = [T u_e \Delta f''(x,0)]^{1/2}, \tag{51.2}$$

$$l = c_\ell\, I(\zeta)^{1/2} \tanh[\kappa\,\zeta/c_\ell], \quad I(\zeta) = 1/(1+5.5\,\zeta^6), \quad c_\ell = 0.085, \tag{51.3}$$

$$l^+ = 1 - \exp(-y^+/A^+), \quad A^+ = A_0^+[1-\exp(-y^+/B^+)]^{1/2}, \quad A_0^+ = 27.8, \quad B^+ = 4.8. \tag{51.4}$$

The expression for l in Eq. (51.3) is a modification of the well-known model by Michel et al. [5], [11] (p. 557), where the usual intermittency factor I by Klebanoff [3] has been included. In turn, the associated pronounced decrease of ℓ eliminates the deficiency of the original model to overestimate the turbulence intensities near the BL edge. The sublayer closure, [1], provided by Eq. (51.4) predicts the correct near-wall behavior given by Eqs. (22).

Formally, Eqs. (51.1)–(51.4) represent an appropriate mixing length closure for r in the fully turbulent case in the double limit $T \to \infty$, $X \to \infty$ if the function $\hat{\rho}(x;k,T)$, introduced in Eq. (51.1), is modelled in a way that $\hat{\rho} \sim \rho$. This behavior then also enforces the transition towards the classical small-defect BL for $T \to \infty$ and $x = O(1)$, where Eqs. (51.3) and (51.4) provide a common overlap of the main and the sublayer, according to Eqs. (26) and (28.2), as $\ell \sim \kappa\zeta$ there. In other words, the model provides the widely believed linear variation of ℓ with distance from the wall in the overlap domain, which is usually argued for by bringing forward dimensional reasoning [11]. Specifically, applying the above model to the "universal" sublayer functions $u_0^+(y^+)$ and $s_0^+(y^+)$ yields $s_0^+ = (\kappa\, y^+ l^+ \mathrm{d}u_0^+/\mathrm{d}y^+)^2$, so that u_0^+ then follows from (numerical) integration of Eq. (25), subject to the no-slip condition $u_0^+(0) = 0$; setting $\kappa = 0.384$ here gives $C^+ \doteq 4.8831$, cf. Eq. (26.2), and $s_0^+ \sim a^+ y^{+3} + O(y^{+7/2})$ with $a^+ \doteq 9.16 \times 10^{-4}$.

Nevertheless, Eqs. (51.1)–(51.4) are aimed to predict the Reynolds stress for all positive values of x, Y, T (and k) with satisfactory accuracy, when the quantities ζ, y^+, κ are identified with those defined in Eqs. (27.1), (30.1), (24) and (26.2). This is accomplished efficiently by fixing the "turbulent" BL edge $\eta = \eta_\infty$ as the minimum value of η where f'' is numerically insignificantly small. Then $\eta_\infty \sim T\delta_1/\Delta$ as $T \to \infty$, and the definition

$$\hat{\rho} := 1/\eta_\infty(x;k,T) \tag{51.5}$$

completes the mixing length closure.

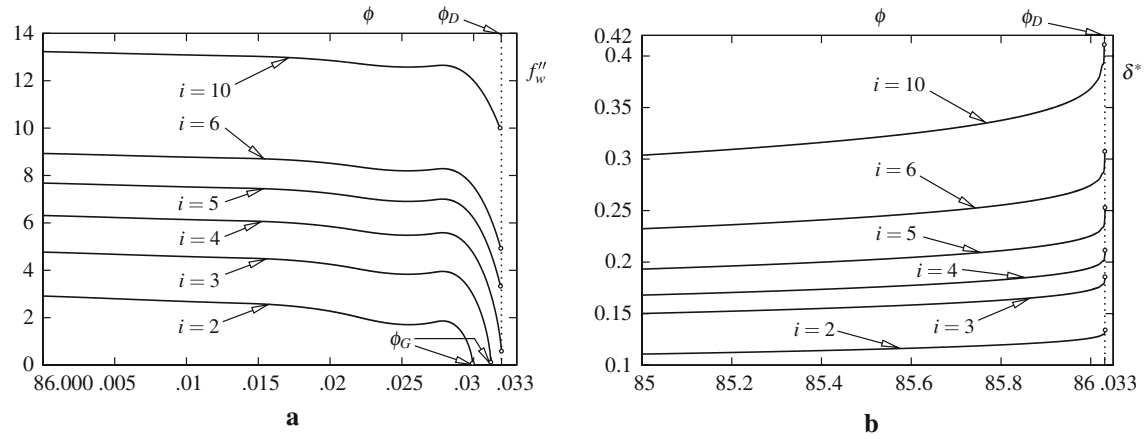

Fig. 3 Numerical solutions of Eqs. (14) and (51), for $k = 0.3$ and $T = i \times 10^4$ over arc angle $\phi\,[^\circ]$ as $\phi - \phi_D(k) \to 0_-$, terminating at $\phi = \phi_G(k, T)$ (positions indicated by *circles*); **a** reduced wall shear stress f''_w, **b** displacement thickness δ^*

6.2 Partially developed turbulent boundary layer near separation

Solutions of the initial-boundary value problem (14), supplemented with Eqs. (51), have been obtained numerically by adopting the method of lines and employing a Keller–Box-type discretization, supplemented with automated adaptive step control in the x-direction. They corroborate the conjecture that the position $x = x_G$ of the Goldstein singularity triggered by the BV singularity, see Eq. (10.2), is shifted downstream for increasing values of k, thereby increasing in strength. Increasing values of T, i.e. increasing turbulence intensities, are expected to foster that downstream shift but, on the other hand, to weaken the strength of the singularity, as turbulent BLs are empirically known to be less prone to separate than the corresponding laminar ones for identical external-flow configurations (i.e. for identical values of k).

This behavior can also be reproduced by calculating solutions for the flow past a circular cylinder with unit radius, as sketched in Fig. 1a, for different values of k and T in a systematic manner, where the potential flow is computed as mentioned briefly in Sect. 3. In order to highlight the consequence of this mechanism, we subsequently discuss solutions of Eqs. (14) for a specific external flow determined by a particular value of k, say, $k = 0.3$. The condition of matching with the external flow in Eq. (14.3) has been satisfied numerically at $\eta = \eta_{\max}$ with $10 \le \eta_{\max} \le 50$, where $\eta_{\max}$ is increased for increasing values of the parameter T. The latter is varied from $T = 0$ up to $T = 10^5$ (higher values result in numerical difficulties which could only be overcome by employing a considerably higher grid resolution). Let $\phi = 180\,x/\pi$ denote the arc angle measured from P_F, see Fig. 2a, hence, the BV singularity is seen to take place at $\phi = \phi_D \doteq 86^\circ\,1'\,54''$, as indicated in Figs. 2b and 3 by vertical dotted lines. The resulting distributions for the reduced wall shear stress and the displacement thickness, given by, respectively, $f''_w := f''(x, 0; k, T)$ and $\delta^*(x; k, T) = \Delta \int_0^\infty (1 - f')\,\mathrm{d}\eta$, are plotted in Fig. 3.

For sufficiently small value of T the BL behaves still laminar-like as the corresponding solutions are found to terminate in form of a Goldstein-type singularity at the location, say, $\phi = \phi_G(k, T)$, i.e. at $x = x_G(k, T)$. That is, f''_w and $\delta^*(x; k, T) - \delta^*(x_G; k, T)$, respectively, vary with $\Delta\phi^{1/2}$, here $\Delta\phi = \phi_G - \phi$, to leading order as $\Delta\phi \to 0_+$. Furthermore, $\phi = \phi_G$ approaches $\phi = \phi_D$ for increasing values of T. Eventually, when T assumes a certain value, say $T = T_D(k)$ (here $T_D \times 10^{-4}$ is slightly below 4), $\phi_G(T_D, k) = \phi_D(k)$. In turn, for $T \ge T_D$ the boundary-layer calculations break down at $\phi = \phi_D(k)$, where f''_w exhibits a finite limit. In fact, the numerical results obtained for relatively large values of T strongly suggest a regular local behavior of the solutions. Consequently, the fully turbulent BL obtained in the limit $T \to \infty$ having a velocity defect of $O(1/\ln T)$, would not separate at all. This result is entirely in line with the analytical investigation given in [9], which applies to a turbulent BL with an asymptotically small velocity deficit as $\phi - \phi_D \to 0_-$, i.e. for $x - x_D \to 0_-$.

From this scenario one then infers that for a certain range of values of k (within the interval $0 < k < 0.5$ in case of the circular cylinder, cf. Subsect. 3) the Goldstein singularity vanishes for critical values of T, denoted by $T_c \ge T_D(k)$. On the other hand, a rational flow description of the local separation process requires that (i) $\Delta\phi = 0$ and, simultaneously, (ii) the Goldstein singularity is vanishingly weak, in order to allow for a viscous/inviscid interaction strategy as in the laminar case, cf. [15]. These conditions suggest that the

streamwise extent of the interaction region is asymptotically small in the limit (1). Therefore, we draw (needless to say, with some caution) the remarkable conclusion that in the BL limit, expressed by the problem posed by Eqs. (14), bluff-body separation is (uniquely) described by critical values $k = k_c$ and $T = T_c = T_D(k_c)$, so that both the above requirements (i) and (ii) are satisfied.

6.3 Transition to fully developed turbulent flow

Considering the case $T \to \infty$ discussed in Subsect. 5.3, reliable solutions of Eqs. (29), (30), subject to Eqs. (14.3), (14.4), are difficult to find due to the extreme thinning of the viscous wall layer as $X \to \infty$ and, therefore, presently available only with limited accuracy. As a first step, however, in Fig. 4a we display the satisfactorily accurate solution of the boundary value problem (40), describing the limiting form of the outer layer as $X \to \infty$. Here l^+, see Eq. (51.4), is correctly replaced by 1, such that $S_1 = (l\, H_1'')^2$, and the sufficiently small cut-off value of the computational domain $10^{-5} \le \zeta \le 1$ accounts for the logarithmic singularity, see Eq. (40.2).

The mixing length closure given by Eqs. (51) enforces the logarithmic law of the wall in the form of Eq. (40.2) and, in turn, transition to a small-defect BL in the limit $X \to \infty$. Nevertheless, the possibility of a large-defect flow, although discarded in Subsect. 5.3 on grounds of considerations regarding the turbulent dynamics, can be taken into account within the framework of the time-mean analysis if the mixing length constant c_ℓ, see Eq. (51.3), is treated as an asymptotically small parameter of $O(\alpha^{1/2})$. The mixing length closure then yields $S_0 = [(\ell/c_l)H_0'']^2$, where Eqs. (51.1) and (51.3) state that $\ell/c_\ell \sim I^{1/2}$, in the following referred to as case (I), in the outermost region of the BL. Although not rigorously justified asymptotically, it is instructive and physically appealing to ascertain the approach of a small velocity defect in the limit (1) by considering numerical solutions $[H_0, S_0](\zeta; \hat\gamma)$ of Eq. (32) that are parametrized by the appropriate coupling parameter

$$\hat\gamma := \gamma_1/c_\ell = O(1), \quad \gamma_1 := \kappa\sigma, \tag{52}$$

see Eq. (35) and the definition of σ in (27.2). Moreover, the match of these self-similar solutions with the then emerging intermediate layer, located between the viscous wall and the main layer and having a thickness of $O(c_\ell^3)$, i.e. of $O(\alpha^{3/2})$, reveals the missing boundary condition $S_0(0; \hat\gamma) = 1$. The latter also holds if a direct match with the viscous wall layer is anticipated, such that the outer and the intermediate layer are treated as a single flow region and, therefore, ℓ is identified with l. Subsequently, this procedure corresponds to case (II).

In addition, since $\alpha = \gamma^2$, Eq. (12) states that $T \sim \gamma_1^2 Re^{1/2}$. From Eqs. (33) and (41) and the definition of δ_1 given by Eq. (27.1) then follows that $\delta_1/x \sim \delta/(\gamma\, x) \sim \gamma\, a(\hat\gamma)$ as $x \to 0$. The results for the thereby (i.e. by the asymptotic theory) expected slope of the BL thickness, $\gamma_1 a(\hat\gamma)$, the suitably defined velocity defect $[1 - H_0'(\zeta; \hat\gamma)]/\gamma$, and the Reynolds shear stress $S_0(\zeta; \hat\gamma)$ are presented in Fig. 4b and Table 1 for different values of $\hat\gamma$, given by Eq. (52), or, equivalently, Re, γ_1, and the aforementioned approximation of T,

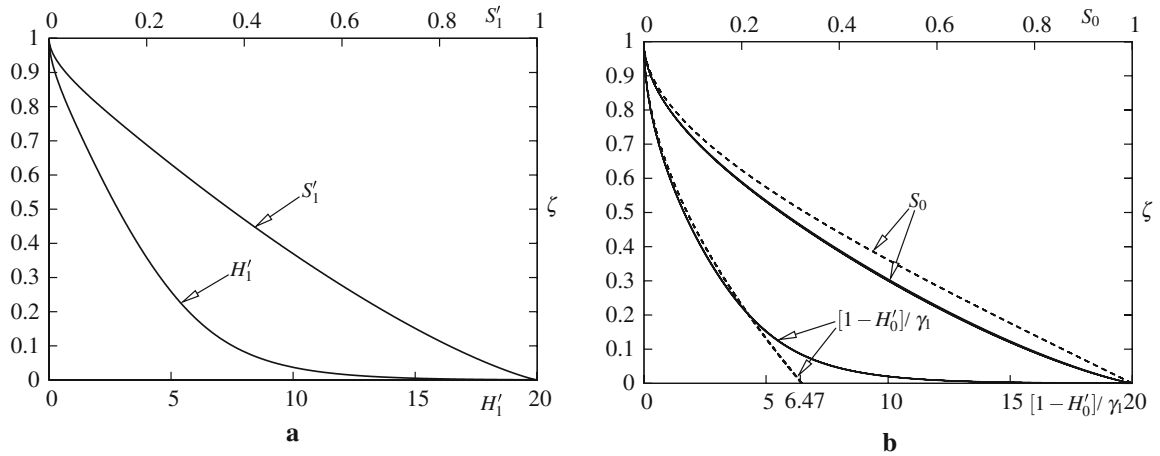

Fig. 4 Numerical solutions of **a** Eqs. (40), giving $\Delta_1 \doteq 0.071658$, $H_1(1) \doteq 3.4888$, and **b** Eq. (32), supplemented with the boundary condition $S_0(0; \hat\gamma) = 1$, for the values of Re given in Table 1

Table 1 Key quantities (rounded values) of the family of solutions of Eq. (32), parametrized by Re

$\lg Re$	8	10	12	14	16	18	20
$10 \times \gamma_1$	0.20846	0.16677	0.13897	0.11912	0.10423	0.09265	0.08338
$T \sim \gamma_1^2 Re^{1/2}$	4.3	27.8	193.1	1419	10864	85839	695298
$\hat{\gamma}$	0.24525	0.19620	0.16350	0.14014	0.12262	0.10900	0.09810
case (I):							
$\gamma_1 a$	0.11775	0.11633	0.11541	0.11476	0.11427	0.11390	0.11360
$H_0'(0;\hat{\gamma})$	0.86491	0.89200	0.91003	0.92291	0.93256	0.94006	0.94607
$[1 - H_0'(0;\hat{\gamma})]/\gamma_1$	6.48057	6.47632	6.47358	6.47165	6.47022	6.46912	6.46824
case (II):							
$\gamma_1 a$	0.10926	0.10757	0.10647	0.10571	0.10514	0.10471	0.10436

respectively: in both the cases (A) and (B), the data exhibit a remarkable collapse, even for moderate values of $\lg Re$. The congruence with the asymptotic limits $[H_1, S_1](\zeta)$, shown in Fig. 4a, becomes more pronounced for increasing values of Re (i.e. decreasing values of $\hat{\gamma}$, as one might expect). In fact, the results clearly indicate that $[H_0'(0;\hat{\gamma}),\ a(\hat{\gamma})] \to [1, \infty]$ as $Re \to \infty$, whereas the latter limit is associated with a rather slow convergence $\gamma a \to \Delta_1$, as indicated by the decreasing values of $\gamma_1 a$. Note the arithmetic mean value of the defect of the slip velocity, $[1 - H_0'(0;\hat{\gamma})]/\hat{\gamma} \approx 6.4728$; accordingly, it is found that $\gamma_1 a \approx 0.11515$ in case (I) and $\gamma_1 a \approx 0.10618$ in case (II), respectively. We mention that good agreement of the corresponding results for the class of self-preserving BLs subject to an adverse pressure gradient and having a velocity defect of $O(1)$ with their strictly asymptotically predicted counterparts, showing a velocity defect of $O(\gamma)$, has already been observed by Melnik [4].

The aforementioned transitional flow taking place where $X = O(1)$ is conveniently described in terms of $[H, S](X, \zeta)$ rather than $[F, R](X, \eta)$, see Eqs. (29.1) and (30.1). This choice of the variables advantageously captures the expected pronounced increase of the BL thickness for large values of X. In order to allow for a comparison of the numerical results with the fully turbulent limiting solution $[H_1, S_1](\zeta)$ that is assumed for $X \to \infty$, we introduce a "defect scaling" by redefining the quantities $\gamma_H(X)$, $\rho(X)$, and $\Delta^+(X)$, originally introduced as gauge functions in Eq. (46) where X is considered to be large, in a suitable form valid for $X \geq 0$,

$$\hat{H}(X,\zeta) := (H-1)/\gamma_H, \quad \hat{S}(X,\zeta) := S/\gamma_H^2, \tag{53.1}$$

$$\gamma_H(X) := -\left[\frac{2}{\kappa}\ln\left(e^{\kappa/2}X+1\right)+1\right]^{-1}, \quad \rho(X) := \frac{1}{1-\Delta_1 X\hat{\gamma}_H}, \quad \Delta^+(X) := \frac{1+X}{\Delta_1+X}\Delta_1\rho^2. \tag{53.2}$$

The scaling provided by Eq. (53.2) not only properly accounts for the limit $X \to \infty$, expressed in Eq. (46) in the case $\Gamma = 1/\Delta_1$ that conforms to a match with the flow downstream. It also allows for a smooth transition of the solution $[H, S](X, \zeta)$] of Eq. (30.2) for $X \to 0$ towards the Hiemenz flow solution.

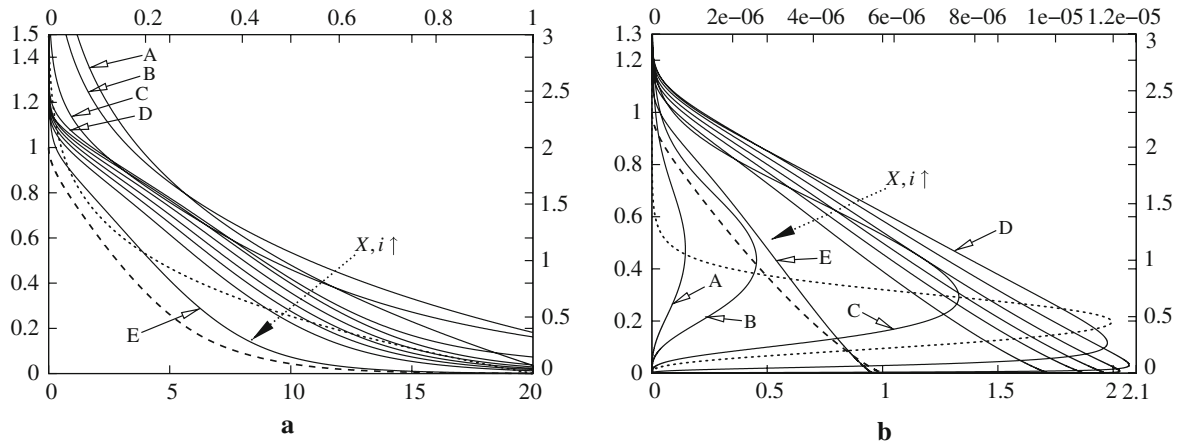

Fig. 5 Distributions for **a** $\hat{H}(X_i, \zeta)$ and **b** $\hat{S}(X_i, \zeta)$, ζ-values indicated by abscissae, values of $\hat{H}$, $\hat{S}$ by ordinates; top abscissae, right ordinates: $X = i = 0$ (Hiemenz solution, *dotted*); bottom abscissae, left ordinates: curves A–D corresponding to $i = 1$–4, curves in order of direction of *dotted arrows* to $i = 5$–9, curves E to $i = 10$, *dashed curves* to $H_1(\zeta)$, $S_1(\zeta)$

Hence, we have solved Eq. (30.2) numerically, subject to the boundary and initial conditions (14.3) and (14.4), where in the latter relationships η, $f(\eta)$, and $f_0(\eta)$ are considered to be formally replaced by ζ and $H(0,\zeta)$. Furthermore, here $S=(\ell H'')^2$, where ℓ is given by Eqs. (51.1)–(51.4). Again, the method already explained briefly at the beginning of Subsect. 6.2 has been adopted. The values of ζ vary from 0 to 3. A very accurate solution of the Hiemenz flow problem (14.4), yielding $[H,S](0,\zeta)$, has been obtained by using 1,500 grid points; the subsequent downstream integration of Eq. (30.2) has been carried out by employing further adaptive grid refinement, specifically close to $\zeta=0$, in order to resolve the thin viscous wall layer that emerges as X becomes large. The resulting profiles $[\hat{H},\hat{S}](X_i,\zeta)$, $i=0,1,\ldots,10$, where $X_0=0$ and $X_i=X_1\exp[(i/10)\ln(X_{10}/X_1)]$ for $i=1,2,\ldots,10$, $X_1=100$, $X_{10}=4\times10^6$, are shown in Fig. 5, together with the limiting solution $[H_1,S_1](\zeta)$. The here chosen exponential increase of the specified values of X accounts for the rather slow rate of convergence of the limit process $[\hat{H},\hat{S}](X,\zeta)\to[H_1,S_1](\zeta)$ as $X\to\infty$, due to the logarithmic dependence of the scaling function $\gamma(X)$ on X, cf. Eqs. (53.2) and (46). However, culminating round-off errors result in the above indicated numerical difficulties for X being large and, thus, make the in Fig. 5 indicated near-collapse of the solution for $i=10$ with the profiles $[H_1,S_1](\zeta)$ only conditionally reliable. Also, progressing further downstream by using the current implementation of the numerical method provokes a breakdown of the computations, even for considerably higher grid resolutions.

7 Conclusions and further outlook

The analysis presented so far indicates that neither the assumption of a purely laminar nor a fully turbulent description of a BL evolving from the front stagnation point provide a concept which is feasible to develop a rational description of break-away separation in the limit (1). Therefore, the global complex asymptotic structure of the flow past a bluff body is characterized by a certain level of the turbulence intensities in its attached part. Most interesting, as a consequence of the occurrence of the front stagnation point P_F, cf. Fig. 1, that level, measured by T, is essentially independent of Re: in the limit $T\to\infty$ close to P_F a small region of streamwise extent of $O(1/T)$ accounts for the transition process of the well-known laminar stagnating flow (Hiemenz flow) towards a fully developed turbulent BL flow of the classical two-layer type. However, as strongly substantiated by the numerical results presented in Subsect. 6.2, a rational description of the flow close to separation is severely hampered by the existence of the small streamwise velocity deficit characterizing the outer main part of that BL. As a result, within the framework of BL theory, the (unique) solution to the global flow problem is presumably provided by the solution of Eqs. (14) for a specific choice of the values of both k and T. It is the objective of a currently performed analytical investigation, tied in with that outlined in [7], to rigorously confirm that the classical turbulent BL structure provides no appropriate basis for establishing a local theory of separation. Also, the local qualitative dependence of the solutions on k and T deduced from the numerical results presented in Subsect. 6.2 should be confirmed by a more extensive careful numerical study of Eqs. (14) and (29.2).

A first answer to the question raised in the paper title can now be given as follows: As a consequence of the scaling of the Reynolds shear stress introduced by Eqs. (11) and (12), the BL never attains a fully developed turbulent state, even for $T\to\infty$. That is, the distinguished limit expressed by Eqs. (47.1) and (47.2), originally believed to accompany short-scale transition near P_F towards a fully developed turbulent BL, should be revised in the form given by Eq. (50) in ensuing studies on this topic. Most important, in this presently undetermined form it is still associated with a BL having a velocity defect of $O(1/\ln T)$ along the surface of a bluff body. The associated asymptotic scaling of that BL is described by Eqs. (48.1), rather than by Eqs. (27.1), which govern fully developed turbulent flow. However, the above outlined current status of our knowledge of the asymptotic flow structure near separation suggests that this slightly "underdeveloped" turbulent BL flow is expected to apply only (i) to relatively slender bodies where the BV singularity encountered in the potential flow is correspondingly weak, cf. [15], leading to a laminar-type separation mechanism of the wall-layer flow, or (ii) presumably to an accordingly revised model of bluff-body separation taking place close to the trailing-edge point P_R, cf. Fig. 1, as proposed originally by Neish and Smith [6], cf. [7]. Noteworthy, from matching of the expansions given by Eqs. (27.1) and (31) it is found that the downstream evolution of the transitional BL, emerging for $x=O(1/T)$, as formulated by Eqs. (29), is associated with a specific member of the class of fully turbulent self-preserving BLs, cf. [11]. Hence, the flow governed by Eqs. (30.1) and (40) is considered as the asymptotically correctly described turbulent counterpart to the purely laminar stagnating flow, here expressed by Eq. (14.4); both this limiting turbulent and the possible transitional solution are presented in Figs. 4 and 5, respectively.

Finally, we note that the analysis of the case $T \to \infty$ carried out here can likely be adopted to allow for a rational description of transition of a BL along a flat plate. In analogy to the case of stagnating flow considered here, transition of the Blasius BL is expected to take place close to the leading edge in the limit (1).

Acknowledgements Special thanks are due to Professor Frank T. Smith (Department of Mathematics, University College London) for frank and stimulating discussions.

References

1. Grifoll, J., Giralt, F.: The near wall mixing length revisited. Int. J. Heat Mass Tran. **43**(19), Technical Note, 3743–3746 (2000)
2. Gurevich, M.I.: The theory of jets in an ideal Fluid. Int. Series of monographs in pure and applied mathematics, vol. 93. Pergamon Press, Oxford (1966). Original Russian book: Fizmatlit, Moscow (1961)
3. Klebanoff, P.S.: Characteristics of turbulence in a boundary layer with zero pressure gradient. NACA Report 1247 (1955) [See also: NACA Technical Note 3178, (1954)]
4. Melnik, R.E.: An asymptotic theory of turbulent separation. Comput. Fluids. **17**(1), 165–184 (1989)
5. Michel, R., Quémard, C., Durant, R.: Hypothesis on the mixing length and application to the calculation of the turbulent boundary layers. In: Kline, S.J., Morkovin, M.V., Sovran, G., Cockrell, D.J. (eds.) Proceedings of Computation of Turbulent Boundary Layers—1968 AFOSR-IFP-Stanford Conference, vol. I: Methods, Predictions, Evaluation and Flow Structure, pp. 195–207. Stanford University, Stanford (1969)
6. Neish, A., Smith, F.T.: On turbulent separation in the flow past a bluff body. J. Fluid Mech. **241**, 443–467 (1992)
7. Scheichl, B., Kluwick, A.: Asymptotic theory of bluff-body separation: a novel shear-layer scaling deduced from an investigation of the unsteady motion. J. Fluids Struct. (2008, in print) [See also in: Unsteady Separated Flows and their Control. In: Braza, M., et al. (eds.) Proceedings of the IUTAM Symposium held in Dassia, Corfu Island, Greece, June 18–22, 2007. Springer-Verlag, Dordrecht (2008, in print)]
8. Scheichl, B., Kluwick, A.: On turbulent marginal boundary layer separation: how the half-power law supersedes the logarithmic law of the wall. Int. J. Comp. Sci. Math. (IJCSM) **1**(2/3/4), 343–359 (2007)
9. Scheichl, B., Kluwick, A.: Turbulent shear-layer scaling in the limit of infinite Reynolds number derived from the unsteady equations of motion. Proc. Appl. Math. Mech. (PAMM) **7**(1) (2007, in press), doi:10.1002/pamm.200700526
10. Schewe, G.: Reynolds-number effects in flows around more-or-less bluff bodies. J. Wind Eng. Ind. Aerod. **89**(14), 1267–1289 (2001)
11. Schlichting, H., Gersten, K.: Boundary-Layer Theory, 8th edn. Springer-Verlag, Berlin (2000)
12. Smith, F.T.: The laminar separation of an incompressible fluid streaming past a smooth surface. Proc. R. Soc. Lond. A **356**(1687), 443–463 (1977)
13. Southwell, R.V., F.R.S., Vaisey, G.: Relaxation methods applied to engineering problems. XII. Fluid motions characterised by 'free' streamlines. Phil. Trans. R. Soc. Lond. A **240**(815), 117–161 (1946)
14. Sychev, V.V.: Laminar Separation. Fluid Dyn. **7**(3), 407–417 (1972). Original Russian article In: Izv. Akad. Nauk SSSR, Mekh. Zhidk. i Gaza (3), 47–59 (1972)
15. Sychev, V.V., Ruban, A.I., Sychev, Vic. V., Korolev, G.L.: Asymptotic Theory of Separated Flows. In: Messiter, A.F., Van Dyke, M., (eds.) Cambridge University Press, Cambridge (1998)
16. Tsahalis, D.T., Telionis, D.P.: On the behavior of turbulent boundary layers near separation. AIAA J. **13**(10), Synoptics, 1261–1262 (1975)
17. Zdravkovich, M.M.: Flow Around Circular cylinders. A Comprehensive Guide Through Flow Phenomena, Experiments, Applications, Mathematical Models, and Computer Simulations, vol. 1: Fundamentals. Oxford University Press, Oxford (1997)